
Discrete Probabilistic Inference as Control in Multi-path Environments

Tristan Deleu¹ Padideh Nouri² Nikolay Malkin¹
 Doina Precup^{2,3} Yoshua Bengio¹
 Mila – Quebec AI Institute

Abstract

We consider the problem of sampling from a discrete and structured distribution as a sequential decision problem, where the objective is to find a stochastic policy such that objects are sampled at the end of this sequential process proportionally to some predefined reward. While we could use maximum entropy Reinforcement Learning (MaxEnt RL) to solve this problem for some distributions, it has been shown that in general, the distribution over states induced by the optimal policy may be biased in cases where there are multiple ways to generate the same object. To address this issue, Generative Flow Networks (GFlowNets) learn a stochastic policy that samples objects proportionally to their reward by approximately enforcing a conservation of flows across the whole Markov Decision Process (MDP). In this paper, we extend recent methods correcting the reward in order to guarantee that the marginal distribution induced by the optimal MaxEnt RL policy is proportional to the original reward, regardless of the structure of the underlying MDP. We also prove that some flow-matching objectives found in the GFlowNet literature are in fact equivalent to well-established MaxEnt RL algorithms with a corrected reward. Finally, we study empirically the performance of multiple MaxEnt RL and GFlowNet algorithms on multiple problems involving sampling from discrete distributions.

1 Introduction

Approximate probabilistic inference has seen a tremendous amount of progress, notably from a variational perspective coupled with deep neural networks. This is particularly true for continuous sample spaces, where the Evidence Lower Bound (ELBO) can be maximized with gradient methods, thanks to methods such as pathwise gradient estimation (Kingma and Welling, 2014; Rezende et al., 2014; Rezende and Mohamed, 2015). In the case of discrete and highly structured sample spaces though, this “reparametrization trick” becomes more challenging since it often requires continuous relaxations of discrete distributions (Jang et al., 2017; Maddison et al., 2017; Mena et al., 2018). In those cases, variational inference can also be carried out more generally thanks to score function estimation (Williams, 1992), albeit at the expense of high variance (Mohamed et al., 2020). An alternative for approximate inference is through sampling methods, based on Markov chain Monte Carlo (MCMC; Hastings, 1970; Gelfand and Smith, 1990), when the target distribution is defined up to an intractable normalization constant.

Bengio et al. (2021) introduced a new class of probabilistic models called *Generative Flow Networks* (GFlowNets), to approximate an unnormalized target distribution over discrete and struc-

¹Université de Montréal, ²McGill University, ³Google DeepMind.

Correspondence: Tristan Deleu (deleutri@mila.quebec)

Code available at: <https://github.com/tristandeleu/gfn-maxent-rl>

tered sample spaces from a variational perspective (Malkin et al., 2023; Zimmermann et al., 2022). GFlowNets treat sampling as a sequential decision making problem, heavily inspired by the literature in Reinforcement Learning (RL). Unlike RL though, which seeks an optimal policy maximizing the cumulative reward, the objective of a GFlowNet is to find a policy such that objects can be sampled proportionally to their cumulative reward. Nevertheless, this relationship led to a number of best practices from the RL literature being transferred into GFlowNets, such as the use of a replay buffer (Shen et al., 2023; Vemgal et al., 2023) and target network (Deleu et al., 2022), and advanced exploration strategies (Rector-Brooks et al., 2023).

Although Bengio et al. (2021) proved that GFlowNets were exactly equivalent to maximum entropy RL (MaxEnt RL; Ziebart, 2010) in some specific cases which we will recall in Section 2, it has long been thought that this connection was only superficial in general. However recently, Tiapkin et al. (2024) showed that GFlowNets and MaxEnt RL are in fact one and the same, up to a correction of the reward function. This, along with other recent works (Mohammadpour et al., 2024; Anonymous, 2023), paved the way to show deeper connections between GFlowNets and MaxEnt RL algorithms. In this work, we extend this correction of the reward to a more general case, and establish novel equivalences between GFlowNet & MaxEnt RL objectives, notably between the widely used Trajectory Balance loss in the GFlowNet literature (Malkin et al., 2022), and the Path Consistency Learning algorithm in MaxEnt RL (Nachum et al., 2017). We also introduce a variant of the Soft Q-Learning algorithm (Haarnoja et al., 2017), depending directly on a policy, and show that it becomes equivalent to the Modified Detailed Balance loss introduced by Deleu et al. (2022). Finally, we show these similarities in behavior empirically on three different domains.

2 Marginal sampling via sequential decision making

Given an energy function $\mathcal{E}(x)$ defined over a discrete and finite sample space \mathcal{X} , our objective is to sample objects $x \in \mathcal{X}$ from the *Gibbs distribution*:

$$P(x) \propto \exp(-\mathcal{E}(x)/\alpha), \quad (1)$$

where $\alpha > 0$ is a temperature parameter. We assume that this energy function is fixed and we can query it for any element in \mathcal{X} . Sampling from this distribution is in general a challenging problem due to the partition function $Z = \sum_{x \in \mathcal{X}} \exp(-\mathcal{E}(x)/\alpha)$ acting as the normalization constant for P , which is intractable when the sample space is (combinatorially) large. Throughout this paper, we will focus on cases where the objects of interest have some compositional structure (*e.g.*, graphs, or trees), meaning that they can be constructed piece by piece.

2.1 Maximum entropy Reinforcement Learning

We consider a finite-horizon Markov Decision Process (MDP) $\mathcal{M}_{\text{soft}} = (\mathcal{S}, \mathcal{A}, s_0, T, r)$, where the state space \mathcal{S} and the action space \mathcal{A} are discrete and finite. We assume that this MDP is deterministic, with a transition function $T : \mathcal{S} \times \mathcal{A} \rightarrow \mathcal{S}$ that determines how to move to a new state $s' = T(s, a)$ from the state s , following the action a . We identify an initial state $s_0 \in \mathcal{S}$ from which all the trajectories start. Moreover, since we are in a finite-horizon setting, all these trajectories are finite and we assume that they eventually end at an abstract terminal state $s_f \notin \mathcal{S}$ acting as a “sink” state. The state space is defined as a superset of the sample space $\mathcal{X} \subseteq \mathcal{S}$, and is structured in such a way that $x \in \mathcal{X}$ iff we can transition from x to the terminal state s_f (*i.e.*, there exists an action $a \in \mathcal{A}$ such that $T(x, a) = s_f$); the states $x \in \mathcal{X}$ are called *terminating states*, following the naming convention of Bengio et al. (2023). We also set the discount factor $\gamma = 1$ throughout this paper.

Since the MDP is deterministic, we can identify the action a leading to a state $s' = T(s, a)$ with the transition $s \rightarrow s'$ in the state space itself. As such, we will write all quantities involving state-action pairs (s, a) in terms of (s, s') instead. The reward function $r(s, s')$ is defined such that the sum of rewards along a complete trajectory (the return) only depends on the energy of the terminating state it reaches: for a trajectory $(s_0, s_1, \dots, s_T, s_f)$, we have

$$\sum_{t=0}^T r(s_t, s_{t+1}) = -\mathcal{E}(s_T), \quad (2)$$

with the convention $s_{T+1} = s_f$. In particular, this covers the case of a sparse reward that is received only at the end of the trajectory (*i.e.*, $r(s_T, s_f) = -\mathcal{E}(s_T)$, and zero everywhere else). This decomposition of the energy into intermediate rewards is similar to Buesing et al. (2020).

While the objective of Reinforcement Learning is typically to find a policy $\pi(s_{t+1} | s_t)$ maximizing the expected sum of rewards (here corresponding to finding a state $x \in \mathcal{X}$ with lowest energy, or equivalently a mode of P in (1)), in *maximum entropy Reinforcement Learning* (MaxEnt RL) we also search for a policy that maximizes the expected sum of rewards, but this time augmented with the entropy $\mathcal{H}(\pi(\cdot | s))$ of the policy π in state s :

$$\pi_{\text{MaxEnt}}^* = \arg \max_{\pi} \sum_{t=0}^T \mathbb{E}_{\tau} [r(s_t, s_{t+1}) + \alpha \mathcal{H}(\pi(\cdot | s_t))]. \quad (3)$$

Notations. In what follows, it will be convenient to view the transitions in this deterministic MDP as a directed acyclic graph (DAG) \mathcal{G} over the states in \mathcal{S} (including s_f), rooted in s_0 ; the graph is acyclic to ensure that $\mathcal{M}_{\text{soft}}$ is finite-horizon. We will use the notations $\text{Pa}(s)$ and $\text{Ch}(s)$ to denote respectively the parents and the children of a state s in \mathcal{G} . For any terminating state $x \in \mathcal{X}$, $s_0 \rightsquigarrow x$ denotes a complete trajectory in \mathcal{G} of the form $\tau = (s_0, s_1, \dots, x, s_f)$; the transition to the terminal state is implicit in the notation, albeit necessary in our definition.

2.2 Sampling terminating states from a soft MDP

From the literature on *control as inference* (Ziebart et al., 2008; Levine, 2018), it can be shown that the policy maximizing the MaxEnt RL objective in (3) induces a distribution over dynamically consistent trajectories $\tau = (s_0, s_1, \dots, s_T, s_f)$ that depends on the sum of rewards along the trajectory:

$$\pi^*(\tau) \triangleq \prod_{t=0}^T \pi_{\text{MaxEnt}}^*(s_{t+1} | s_t) \propto \exp \left(\frac{1}{\alpha} \sum_{t=0}^T r(s_t, s_{t+1}) \right). \quad (4)$$

With our choice of reward function in (2), this suggests a simple strategy to sample from the Gibbs distribution in (1), once the optimal policy π_{MaxEnt}^* is known: sample a trajectory in $\mathcal{M}_{\text{soft}}$, starting at the initial state s_0 and following the optimal policy, and only return the terminating state s_T reached at the end of τ (ignoring the terminal state s_f). However, in general, we are interested in sampling an object $x \in \mathcal{X}$ (the terminating state) using this sequential process, but not *how* this object is generated (the exact trajectory taken). The distribution of interest is therefore not a distribution over *trajectories* as in (4), but its *marginal* over terminating states:

$$\pi^*(x) \triangleq \sum_{\tau: s_0 \rightsquigarrow x} \pi^*(\tau). \quad (5)$$

$\pi^*(x)$ is called the *terminating state distribution* associated with the policy π_{MaxEnt}^* (Bengio et al., 2023). When the state transition graph \mathcal{G} of the soft MDP is a tree¹ rooted in s_0 , and there is a unique complete trajectory $s_0 \rightsquigarrow x$ leading to any $x \in \mathcal{X}$, then this process is guaranteed to be equivalent to sampling from the Gibbs distribution (Bengio et al., 2021). Examples of tree-structured MDPs include the autoregressive generation of sequences (Bachman and Precup, 2015; Weber et al., 2015; Angermueller et al., 2020; Jain et al., 2022; Feng et al., 2022), and sampling from a discrete factor graph with a fixed ordering of the random variables (Buesing et al., 2020).

The equivalence between control and inference, or sampling, no longer holds when \mathcal{G} is a general DAG. As an illustrative example, shown in Figure 1, consider the problem of generating small molecules by adding fragments one at a time, as described in You et al. (2018). If we follow the optimal policy, even though the distribution over trajectories is proportional to $\exp(-\mathcal{E}(x))$ as in (4), its marginal over terminating states is biased since there are two trajectories leading to the same molecule x_4 (i.e., multiple orders in which fragments can be added). This bias was first highlighted by Bengio et al. (2021).

2.3 Generative Flow Networks

To address this mismatch between the target Gibbs distribution in (1) and the terminating state distribution in (5) induced by the optimal policy in MaxEnt RL, Bengio et al. (2021) introduced a new class of probabilistic models over discrete and compositional objects called *Generative Flow Networks* (GFlowNets; Bengio et al., 2023). Instead of searching for a policy maximizing (3), the

¹With the exception of the terminal state s_f , whose parents are always all the terminating states in \mathcal{X} .

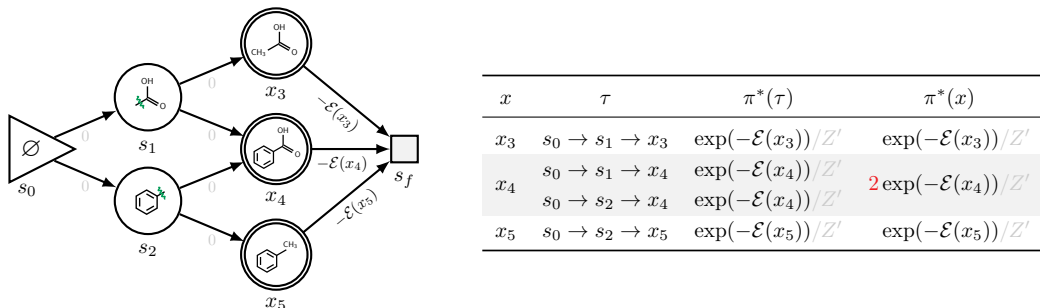


Figure 1: Illustration of the bias of the terminating state distribution associated with π_{MaxEnt}^* on a soft MDP with a DAG structure. The labels on each transition of the MDP corresponds to the reward function, satisfying (2) (sparse reward setting). The terminating state distribution $\pi^*(x)$ is computed by marginalizing $\pi^*(\tau)$ over trajectories leading to x (e.g., two trajectories $s_0 \rightarrow s_1 \rightarrow x_4$ and $s_0 \rightarrow s_2 \rightarrow x_4$ to x_4). $\pi^*(\tau)$ is computed based on (4), and we assume $\alpha = 1$. The terminating state distribution $\pi^*(x)$ should be contrasted with the (target) Gibbs distribution $P(x) \propto \exp(-\mathcal{E}(x))$. The normalization constant is $Z' = \exp(-\mathcal{E}(x_3)) + 2 \exp(-\mathcal{E}(x_4)) + \exp(-\mathcal{E}(x_5))$. This MDP is inspired by Jain et al. (2023a).

goal of a GFlowNet is to find a *flow* function $F(s \rightarrow s')$ defined over the edges of \mathcal{G} that satisfies the following flow-matching conditions for all states $s' \in \mathcal{S}$ such that $s' \neq s_0$:

$$\sum_{s \in \text{Pa}(s')} F(s \rightarrow s') = \sum_{s'' \in \text{Ch}(s')} F(s' \rightarrow s''), \quad (6)$$

with an additional boundary condition $F(x \rightarrow s_f) = \exp(-\mathcal{E}(x)/\alpha)$ for each terminating state $x \in \mathcal{X}$. Putting it in words, (6) means that the total amount of flow going into any state s' has to be equal to the amount of flow going out of it, except for the initial state s_0 which acts as a single “source” for all the flow. We can define a policy² from a flow function by simply normalizing the flows going out of any state s_t :

$$P_F(s_{t+1} | s_t) \propto F(s_t \rightarrow s_{t+1}). \quad (7)$$

Bengio et al. (2021) showed that if there exists a flow function satisfying the flow-matching conditions in (6) as well as the boundary conditions, then sampling terminating states by following P_F in the soft MDP as described in Section 2.2 is equivalent to sampling from the Gibbs distribution in (1). In that case, the terminating state distribution associated with the policy P_F satisfies $P_F(x) \propto \exp(-\mathcal{E}(x)/\alpha)$, for any terminating state $x \in \mathcal{X}$, and is not biased by the number of trajectory leading to x , contrary to the optimal policy in MaxEnt RL.

3 Bridging the gap between MaxEnt RL & GFlowNets

There exists a fundamental difference between MaxEnt RL and GFlowNets in the way the distributions induced by their (optimal) policies relate to the energy: in MaxEnt RL, this distribution is over *how* objects are being created (trajectories) as mentioned in Section 2.2, whereas a GFlowNet induces a distribution over the *outcomes* only (terminating states), the latter matching the requirements of the Gibbs distribution. In this section, we recall some existing connections between GFlowNets and MaxEnt RL (Tiapkin et al., 2024), and we establish new equivalences between existing MaxEnt RL algorithms and GFlowNet objectives.

3.1 Reward correction

To correct the bias illustrated in Figure 1 caused by multiple trajectories leading to the same terminating state, we can treat (5) not as a sum but as an *expectation* over trajectories, by reweighing

²Following the conventions from the GFlowNet literature, we will use the notation P_F for this policy, also called the forward transition probability (Bengio et al., 2023), to distinguish it from the optimal policy π_{MaxEnt}^* in MaxEnt RL.

$\pi^*(\tau)$ (which is constant for a fixed terminating state, by (4) & (2)) with a probability distribution over these trajectories. Bengio et al. (2023) showed that such a distribution over complete trajectories can be defined by introducing a *backward transition probability* $P_B(s | s')$, which is a distribution over the parents $s \in \text{Pa}(s')$ of any state $s' \neq s_0$. Tiapkin et al. (2024) showed that the reward of the soft MDP can be modified based on P_B in such a way that the corresponding optimal policy π_{MaxEnt}^* is equal to the GFlowNet policy P_F in (7). We restate and generalize this result in Theorem 3.1, where we show how this correction counteracts the effect of the marginalization in (5), resulting in a terminating state distribution that matches the Gibbs distribution.

Theorem 3.1 (Gen. of Tiapkin et al., 2024; Theorem 1). *Let $P_B(\cdot | s')$ be an arbitrary backward transition probability (i.e., a distribution over the parents of $s' \neq s_0$ in \mathcal{G}). Let $r(s, s')$ be the reward function of the MDP corrected with P_B , satisfying for any trajectory $\tau = (s_0, s_1, \dots, s_T, s_f)$:*

$$\sum_{t=0}^T r(s_t, s_{t+1}) = -\mathcal{E}(s_T) + \alpha \sum_{t=0}^{T-1} \log P_B(s_t | s_{t+1}), \quad (8)$$

where we used the convention $s_{T+1} = s_f$. Then the terminating state distribution associated with the optimal policy π_{MaxEnt}^* solution of (3) satisfies $\pi^*(x) \propto \exp(-\mathcal{E}(x)/\alpha)$.

The proof of the theorem is available in Appendix A. Unlike (2), the return now depends on the trajectory leading to s_T via the second term in (8). Interestingly, the temperature parameter α introduced in the MaxEnt RL literature (Haarnoja et al., 2017) finds a natural interpretation as the temperature of the Gibbs distribution. Note that the correction in (8) only involves the backward probability of the whole trajectory τ , making it also compatible even with non-Markovian P_B (Shen et al., 2023; Bengio et al., 2023).

Tiapkin et al. (2024) only considered the case where the reward function of the soft MDP is sparse, and the correction with $P_B(s_t | s_{t+1})$ is added at each intermediate transition $s_t \rightarrow s_{t+1}$; we will go back to this setting in the following section. This correction of the reward is fully compatible with our observation in Section 2.2 that sampling terminating states with π_{MaxEnt}^* yields samples of (1) when the soft MDP is a tree with the (uncorrected) reward in (2), since in that case any state $s' \neq s_0$ has a unique parent s , and thus $P_B(s | s') = 1$ as also observed by Tiapkin et al. (2024).

3.2 Equivalence between Path Consistency Learning & (Sub-)Trajectory Balance

Similar to how (2) covered the particular case of a sparse reward, in this section we will consider a reward function satisfying (8) where the energy function only appears at the end of the trajectory

$$r(s_t, s_{t+1}) = \alpha \log P_B(s_t | s_{t+1}) \quad r(s_T, s_f) = -\mathcal{E}(s_T), \quad (9)$$

as introduced in (Tiapkin et al., 2024). Theorem 3.1 suggests that solving the MaxEnt RL problem in (3) with the corrected reward is comparable to finding a solution of a GFlowNet, as they both lead to a policy whose terminating state distribution is the Gibbs distribution. It turns out that there exists an equivalence between specific algorithms solving these two problems with our choice of reward function above: Path Consistency Learning (PCL; Nachum et al., 2017) for MaxEnt RL, and the Sub-trajectory Balance objective (SubTB; Madan et al., 2023; Malkin et al., 2022) for GFlowNets. Both of these objectives operate at the level of partial trajectories of the form $\tau = (s_m, s_{m+1}, \dots, s_n)$, where s_m and s_n are not necessarily the initial and terminal states anymore.

On the one hand, the PCL objective $\mathcal{L}_{\text{PCL}}(\theta, \phi) = \frac{1}{2} \mathbb{E}_{\pi_b} [\Delta_{\text{PCL}}^2(\tau; \theta, \phi)]$ encourages the consistency between a policy π_θ parametrized by θ and a soft value function V_{soft}^ϕ parametrized by ϕ , where π_b is an arbitrary distribution over (partial) trajectories τ , and the residual is defined as

$$\Delta_{\text{PCL}}(\tau; \theta, \phi) = -V_{\text{soft}}^\phi(s_m) + V_{\text{soft}}^\phi(s_n) + \sum_{t=m}^{n-1} (r(s_t, s_{t+1}) - \alpha \log \pi_\theta(s_{t+1} | s_t)). \quad (10)$$

On the other hand, the SubTB objective $\mathcal{L}_{\text{SubTB}}(\theta, \phi) = \frac{1}{2} \mathbb{E}_{\pi_b} [\Delta_{\text{SubTB}}^2(\tau; \theta, \phi)]$ also enforces some form of consistency, but this time between a policy (forward transition probability) P_F^θ parametrized by θ , and a state flow function F_ϕ parametrized by ϕ , and the residual is defined as

$$\Delta_{\text{SubTB}}(\tau; \theta, \phi) = \log \frac{F_\phi(s_n) \prod_{t=m}^{n-1} P_B(s_t | s_{t+1})}{F_\phi(s_m) \prod_{t=m}^{n-1} P_F^\theta(s_{t+1} | s_t)}, \quad (11)$$

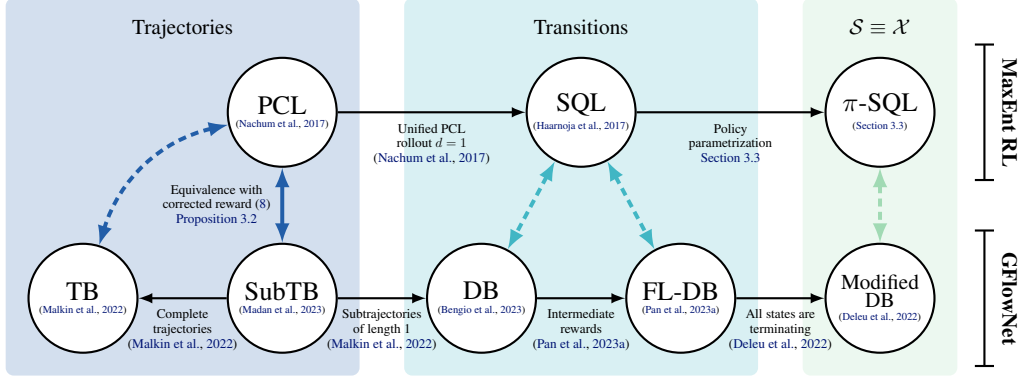


Figure 2: Equivalence between the objectives of MaxEnt RL algorithms, with corrected rewards defined in (9), and the objectives in GFlowNets.

where P_B is a backward transition probability, which we assume to be fixed here—although in general, P_B may also be learned (Malkin et al., 2022). In addition to this objective, some boundary conditions on F_ϕ must also be enforced (depending on \mathcal{E}), similar to the ones introduced in Section 2.3; see Appendix B.1 for details. The following proposition establishes the equivalence between these two objectives, up to a normalization constant that only depends on the temperature α , and provides a way to move from the policy/value function parametrization in MaxEnt RL to the policy/flow function parametrization in GFlowNets. Although similarities between these two methods have been mentioned in prior work (Malkin et al., 2022; Jiralerspong et al., 2024; Hu et al., 2024; Mohammadpour et al., 2024), we show here an exact equivalence between both objectives.

Proposition 3.2. *The Subtrajectory Balance objective (GFlowNet; Madan et al., 2023) is proportional to the Path Consistency Learning objective (MaxEnt RL; Nachum et al., 2017) on the soft MDP with the reward function defined in (9), in the sense that $\mathcal{L}_{\text{PCL}}(\theta, \phi) = \alpha^2 \mathcal{L}_{\text{SubTB}}(\theta, \phi)$, with the following correspondence*

$$\pi_\theta(s' | s) = P_F^\theta(s' | s) \quad V_{\text{soft}}^\phi(s) = \alpha \log F_\phi(s). \quad (12)$$

The proof of this proposition is available in Appendix B.1. The equivalence between the value function in MaxEnt RL and the state flow function in GFlowNets was also found in (Tiapkin et al., 2024). When applied to complete trajectories, this also shows the connection between the Trajectory Balance objective (TB; Malkin et al., 2022), widely used in the GFlowNet literature, and PCL under our choice of corrected reward in (9).

On the other end of the spectrum, if we apply this proposition to transitions in the soft MDP (*i.e.*, subtrajectories of length 1), then we can obtain a similar equivalence between the Detailed Balance objective in GFlowNets (DB; Bengio et al., 2023), and the Soft Q-Learning algorithm (SQL; Haarnoja et al., 2017), via the *Unified PCL* perspective of Nachum et al. (2017) that uses a soft Q-function in order to simultaneously parametrize both the policy and the value function in (10); see Corollary B.1 for a detailed statement. We note that this connection between DB & SQL was also mentioned in prior work (Tiapkin et al., 2024; Mohammadpour et al., 2024). A full summary of the connections resulting from Proposition 3.2 between different MaxEnt RL and GFlowNet objectives is available in Figure 2, with further details in Figure 6.

3.3 Soft Q-Learning with policy parametrization

In this section, we consider the case where all the states of the soft MDP are valid elements of the sample space \mathcal{X} (in other words, all the states are terminating). Since every state is now associated with some energy, we can reshape the rewards (Ng et al., 1999) while still satisfying (8) as

$$r(s_t, s_{t+1}) = \mathcal{E}(s_t) - \mathcal{E}(s_{t+1}) + \alpha \log P_B(s_t | s_{t+1}) \quad r(s_T, s_f) = 0, \quad (13)$$

if we assume, without loss of generality, that $\mathcal{E}(s_0) = 0$ (any offset added to the energy function leaves (1) unchanged). This is a novel setting that differs from Tiapkin et al. (2024), and was made possible thanks to our general statement in Theorem 3.1. We show in Proposition B.2 that with our

choice of rewards above, in particular the fact that no reward is received upon termination, we can express the objective of Soft Q-Learning as a function of a policy π_θ parametrized by θ , instead of a Q-function; we call this π -SQL. The objective can be written as $\mathcal{L}_{\pi\text{-SQL}}(\theta) = \frac{1}{2}\mathbb{E}_{\pi_b}[\Delta_{\pi\text{-SQL}}^2(s, s'; \theta)]$, where π_b is an arbitrary distribution over transitions $s \rightarrow s'$ such that $s' \neq s_f$, and

$$\Delta_{\pi\text{-SQL}}(s, s'; \theta) = \alpha [\log \pi_\theta(s' | s) - \log \pi_\theta(s_f | s) + \log \pi_\theta(s_f | s')] - r(s, s'). \quad (14)$$

With the reward function in (13), this alternative perspective on SQL is remarkable in that it is equivalent to the Modified Detailed Balance objective (Modified DB; Deleu et al., 2022), specifically derived in the special case of GFlowNets whose states are all terminating. This objective can be written as $\mathcal{L}_{\text{M-DB}}(\theta) = \frac{1}{2}\mathbb{E}_{\pi_b}[\Delta_{\text{M-DB}}^2(s, s'; \theta)]$ that depends on a policy (forward transition probability) P_F^θ parametrized by θ , where

$$\Delta_{\text{M-DB}}(s, s'; \theta) = \log \frac{\exp(-\mathcal{E}(s')/\alpha)P_B(s | s')P_F^\theta(s_f | s)}{\exp(-\mathcal{E}(s)/\alpha)P_F^\theta(s' | s)P_F^\theta(s_f | s')}. \quad (15)$$

Proposition 3.3. *Suppose that all the states of the soft MDP are terminating $\mathcal{S} \equiv \mathcal{X}$. The Modified Detailed Balance objective (GFlowNet; Deleu et al., 2022) is proportional to the Soft Q-Learning objective with a policy parametrization (MaxEnt RL; π -SQL) on the soft MDP with the reward function defined in (13), in the sense that $\mathcal{L}_{\pi\text{-SQL}}(\theta) = \alpha^2 \mathcal{L}_{\text{M-DB}}(\theta)$, with $\pi_\theta(s' | s) = P_F^\theta(s' | s)$.*

The proof is available in Appendix B.3. This result can be further generalized to cases where the states are not necessarily all terminating, but where some partial reward can be received along the trajectory, with an equivalence between SQL and the Forward-Looking Detailed Balance objective (FL-DB; Pan et al., 2023a) in GFlowNets; see Appendix B.4 for details.

4 Related Work

Maximum Entropy Reinforcement Learning. Unlike standard reinforcement learning where an optimal policy may be completely deterministic (at least in the fully observable case; Sutton and Barto, 2018), MaxEnt RL seeks a *stochastic* policy that balances between reward maximization and maximal entropy of future actions (Ziebart, 2010; Fox et al., 2016). This type of entropy regularization falls into the broader domain of regularized MDPs (Geist et al., 2019). This can be particularly beneficial for improving exploration (Haarnoja et al., 2017) and for robust control under model misspecification (Eysenbach and Levine, 2022). Popular MaxEnt RL methods include Soft Q-Learning, Path Consistency Learning (Nachum et al., 2017), and Soft Actor-Critic (Haarnoja et al., 2018a) studied in this paper.

Generative Flow Networks. Bengio et al. (2021) took inspiration from reinforcement learning and introduced GFlowNets as a solution for finding diverse molecules binding to a target protein. Since then, they have found applications in a number of domains in scientific discovery (Jain et al., 2022, 2023a; Mila AI4Science et al., 2023), leveraging diversity in conjunction with active learning (Jain et al., 2023b; Hernandez-Garcia et al., 2023), but also in combinatorial optimization (Zhang et al., 2023a,b), causal discovery (Deleu et al., 2022, 2023; Atanackovic et al., 2023), and probabilistic inference in general (Zhang et al., 2022b; Hu et al., 2023, 2024; Falet et al., 2024). Although they were framed differently, GFlowNets are also deeply connected to the literature on variational inference (Malkin et al., 2023; Zimmermann et al., 2022).

A number of works have recently alluded to connections between GFlowNets and (maximum entropy) RL. The only work to formally establish the connection is Tiapkin et al. (2024), which showed how the reward in MaxEnt RL can be corrected based on some backward transition probability to be equivalent to GFlowNets. Although their analysis is limited to the case where the reward function in the original soft MDP is sparse (*i.e.*, the reward is only obtained at the end of the trajectory), they were the first to propose a correction applied at each intermediate transition as in Section 3.2. We generalized this in Theorem 3.1 with a correction at the level of the *trajectories*, which offers more flexibility in how the correction is distributed along the trajectory and allows intermediate rewards. Tiapkin et al. (2024) also showed similarities between GFlowNet objectives and MaxEnt RL algorithms, namely between Detailed Balance & Dueling Soft Q-Learning (Wang et al., 2016), and between Trajectory Balance & Policy Gradient (Schulman et al., 2017). The correspondence between

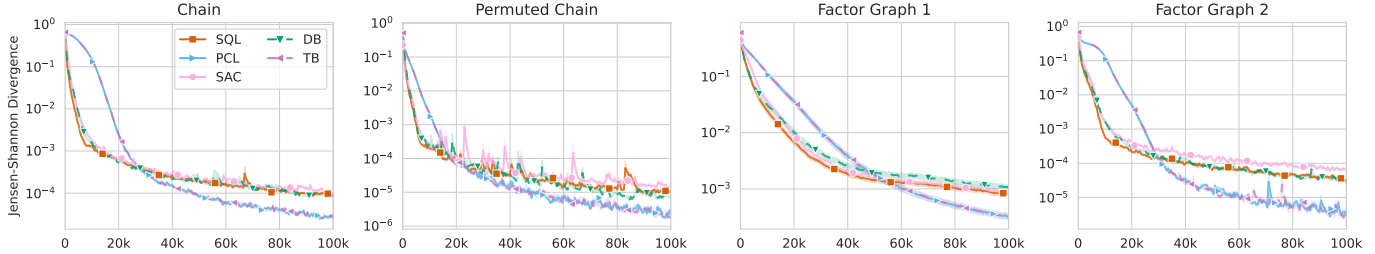


Figure 3: Comparison of MaxEnt RL and GFlowNet algorithms on the factor graph inference task, in terms of the Jensen-Shannon divergence between the terminating state distribution and the target distribution during training. Each curve represents the average JSD with 95% confidence interval over 20 random seeds.

TB and Policy Gradient was further expanded in (Anonymous, 2023), as a direct consequence of the connections between GFlowNets, variational inference (Malkin et al., 2023), and reinforcement learning (Weber et al., 2015). Finally, Mohammadpour et al. (2024) also introduced a correction that depends on $n(s)$ the number of (partial) trajectories to a certain state s , which can be learned by solving a second MaxEnt RL problem (3) on an “inverse” MDP. This correction corresponds to a particular choice of backward transition probability $P_B(s_t | s_{t+1}) = n(s_t)/n(s_{t+1})$ in (8), which has the remarkable property of maximizing the flow entropy.

5 Experimental results

We verify empirically the equivalences established in Section 3 on three domains: the inference over discrete factor graphs (Buesing et al., 2020), Bayesian structure learning of Bayesian networks (Deleu et al., 2022), and the generation of parsimonious phylogenetic trees (Zhou et al., 2024). In addition to Detailed Balance (and possibly its modified version) and Trajectory Balance on the one hand (GFlowNets), and Soft Q-Learning (possibly parametrized by a policy; see Section 3.3) and Path Consistency Learning on the other hand (MaxEnt RL), we also consider a discrete version of Soft Actor-Critic (Christodoulou, 2019), which has no natural counterpart in the GFlowNet literature. For all MaxEnt RL methods, we adjust the MDP to include the correction of the reward. Note that in all the domains considered here, intermediate rewards are available in the original MDP, meaning in particular that all instances of DB actually use the Forward-Looking formulation (Pan et al., 2023a). Additional experimental details are available in App. C.

5.1 Probabilistic inference over discrete factor graphs

The probabilistic inference task in Buesing et al. (2020) consists in sequentially sampling the values of d discrete random variables in a factor graph one at a time, with a fixed order. This makes the underlying MDP having a tree structure, eliminating the need for reward correction, as described in Section 2.2. We adapted this environment to have multiple trajectories leading to each terminating state by allowing sampling the random variables in any order. Details about the energy function are available in Appendix C.1.

In Figure 3, we show the performance of the different MaxEnt RL and GFlowNet algorithms on 4 different factor graph structures, as proposed by Buesing et al. (2020), with $d = 6$ variables and where each variable can take one of 5 possible values. We observe that TB & PCL perform similarly, validating Proposition 3.2, and overall outperform all other methods. Similarly, we can see that DB & SQL also perform similarly as expected by Corollary B.1. Finally, although SAC is generally viewed as a strong algorithm for continuous control (Haarnoja et al., 2018b), we did not observe any significant improvement over DB/SQL.

5.2 Structure learning of Bayesian Networks

We also evaluated all algorithms on the task of learning the structure of Bayesian networks, using a Bayesian perspective (Deleu et al., 2022). Given a dataset of observations \mathcal{D} from a joint distribu-

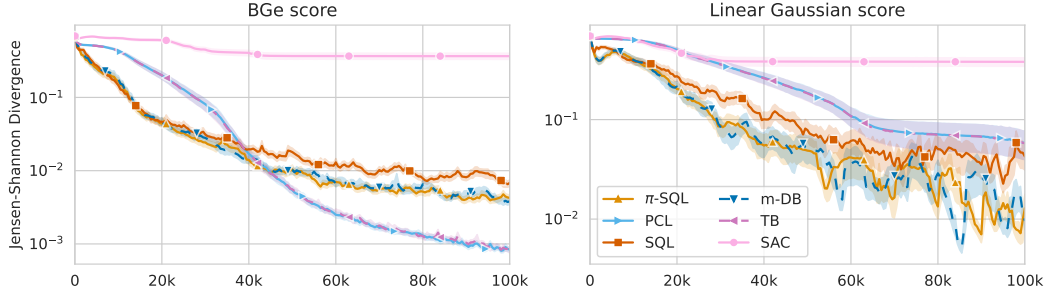


Figure 4: Comparison of MaxEnt RL and GFlowNet algorithms on the Bayesian structure learning task, in terms of the Jensen-Shannon divergence between the terminating state distribution and the target posterior during training. Both experiments differ in the way the marginal likelihood $P(\mathcal{D} | G)$ is computed, (left) using the BGe score (Geiger and Heckerman, 1994), (right) is the linear Gaussian score (Nishikawa-Toomey et al., 2023). Each curve represents the average JSD with 95% confidence interval over 20 random seeds.

tion over d random variables X_1, \dots, X_d , our objective is to approximate the posterior distribution $P(G | \mathcal{D}) \propto P(\mathcal{D} | G)P(G)$ over the DAG structures G encoding the conditional independencies of $P(X_1, \dots, X_d)$. The soft MDP is constructed as in (Deleu et al., 2022), where a DAG G is constructed by adding one edge at a time, starting from a completely empty graph, while enforcing the acyclicity of the graph at each step of generation (*i.e.*, an edge cannot be added if it would introduce a cycle).

Following Malkin et al. (2023), we consider here a relatively small task where $d = 5$, so that the target distribution $P(G | \mathcal{D})$ can be evaluated analytically in order to compare it to our approximations given by MaxEnt RL and/or GFlowNets. Unlike in Section 5.1, we also included the modified DB loss and π -SQL in our comparison since all the states are valid DAGs. We observe in Figure 4 that again TB & PCL on the one hand, but also modified DB & π -SQL on the other hand perform very similarly to one another, empirically validating our equivalences established above. Despite a light search over hyperparameters, we found that SAC performs on average significantly worse than other methods, mainly due to instability during training.

5.3 Phylogenetic tree generation

Finally, we also compared these methods on the larger-scale task of parsimonious phylogenetic tree generation introduced by Zhou et al. (2024). Based on biological sequences of different species, the objective is to find phylogenetic trees over those species that require few mutations. A state of the soft MDP corresponds to a collection of trees over a partition of the species, and actions correspond to merging two trees together by adding a root node. Note that all the trees sampled this way have the same size, although they may have different number of trajectories leading to each of them (unlike Figure 3). The energy of a tree T corresponds to the total number of mutations captured in T .

In Figure 5, we compare the performance of all methods on 6 datasets introduced by Zhou et al. (2024), in terms of the correlation between the terminating state log-probabilities $\log \pi(T)$ associated with the learned policy, and the (uncorrected) return $-\mathcal{E}(T)$, since we should ideally have

$$\log \pi(T) \approx \log \pi^*(T) = -\mathcal{E}(T) - \log Z, \quad (16)$$

based on Theorem 3.1. We observe once again that TB & PCL perform overall similarly to one another, as well as DB & SQL, confirming our observations made above, this time on larger problems where the partition function is intractable. Similar to Section 5.2, we also found that SAC was often less competitive than DB/SQL, except for DS4.

6 Discussion

Stochastic environments. Similar to (Mohammadpour et al., 2024), we note that our results here are limited to the case where the soft MDP is deterministic, to match the standard assumptions

	TB	PCL	DB	SQL	SAC
DS1	0.7797	0.7399	0.9141	0.8695	0.6003
DS2	0.8550	0.8309	0.8811	0.8922	0.7022
DS3	0.5833	0.6137	0.8649	0.8474	0.6334
DS4	0.9178	0.9177	0.9285	0.8965	0.9320
DS5	0.9688	0.9690	0.9633	0.9712	0.9567
DS6	0.9526	0.9542	0.9496	0.9615	0.8017

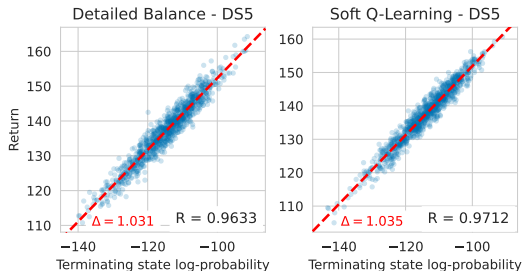


Figure 5: Comparison of MaxEnt RL and GFlowNet algorithms on the phylogenetic tree generation task. (Left) Comparison of the performance in terms of the Pearson correlation between the terminating state log-probability and the return on 1000 randomly sampled trees. (Center) Correlation between the terminating state log-probability found with DB and the return, each point representing a tree, with a best linear fit line and its slope. (Right) Similarly for SQL. The correlation plots for all methods and all datasets are available in [Appendix C.3](#).

made in the GFlowNet literature. Although some works have attempted to generalize GFlowNets to stochastic environments (Bengio et al., 2023; Pan et al., 2023b), there is no apparent consensus on how to guarantee the existence of an optimal policy P_F whose terminating state distribution matches (1) when an object may be generated in multiple ways (*i.e.*, \mathcal{G} is a DAG). Jiralerspong et al. (2024) introduced an extension to stochastic environments called *EFlowNet* where an optimal policy is guaranteed to exist, albeit limited to the case where the soft MDP has a tree structure and would therefore bypass the need for any reward correction. The assumption of determinism is generally not limiting though since the structure of the soft MDP is typically designed by an expert based on the problem at hand (depending on the distribution to be approximated).

Environments with equal number of trajectories. We saw in [Section 2.2](#) that without correcting the reward function, the optimal policy π_{MaxEnt}^* has a terminating state distribution biased towards states with more complete trajectories leading to them. However, there are some situations where *all* the states have an equal number of trajectories leading to them. This is the case of the discrete factor graphs environments studied in [Section 5.1](#) for example, where all terminating states can be accessed with exactly $n!$ trajectories since each of the n variables can be assigned a value in any order. In this situation, one can apply MaxEnt RL with the original reward in (2), without any correction, and still obtain a terminating state distribution equal to the Gibbs distribution, since this constant can be absorbed into the partition function. Just like the case where \mathcal{G} is a tree, this must be considered as a very special case though, and it is generally recommended to always correct the reward with P_B .

Unified parametrization of the policy & state flow. In all applications of GFlowNets involving the SubTB objective (Madan et al., 2023; Malkin et al., 2022) found in the literature, the forward transition probabilities P_F^θ and the state flow function F_ϕ have always been parametrized with separate models (with possibly a shared backbone) as in [Section 3.2](#). However, thanks to the equivalence with PCL established in [Proposition 3.2](#), it is actually possible to parametrize both functions using a single “Q-function” thanks to the Unified PCL perspective (Nachum et al., 2017); see also [Appendix B.2](#) in the context of DB & SQL. A setting with separate networks is closer to the use of a dueling architecture as highlighted by Tiapkin et al. (2024). In our experiments, we observed that using DB with two separate networks performs overall similarly to SQL with a single Q-network, even though the latter requires fewer parameters to learn. A complete study of the effectiveness of this strategy compared to separate networks is left as future work.

Continuous control & probabilistic inference. While this paper focused on discrete distributions, to match the well-studied setting in the GFlowNet literature, the reward correction in [Theorem 3.1](#) may be extended to cases where \mathcal{X} , along with the state and action spaces of the soft MDP, are continuous spaces as conjectured by Tiapkin et al. (2024). We could establish similar connections with MaxEnt RL objectives by leveraging the extensions of GFlowNets to continuous spaces (Li et al., 2023; Lahlou et al., 2023). Interestingly, continuous GFlowNets have strong connections with diffusion models (Zhang et al., 2022a; Sendera et al., 2024), for which RL has been shown to be an effective training method (Fan and Lee, 2023; Black et al., 2023).

Acknowledgements

We would like to thank Valentin Thomas, Michal Valko, Pierre Ménard, Daniil Tiapkin, and Sobhan Mohammadpour for helpful discussions and comments about this paper. This research was enabled in part by compute resources and software provided by Mila (mila.quebec).

References

- Christof Angermueller, David Dohan, David Belanger, Ramya Deshpande, Kevin Murphy, and Lucy Colwell. Model-based reinforcement learning for biological sequence design. *International Conference on Learning Representations*, 2020.
- Anonymous. GFlowNet Training by Policy Gradients. *OpenReview*, 2023.
- Lazar Atanackovic, Alexander Tong, Jason Hartford, Leo J Lee, Bo Wang, and Yoshua Bengio. DynGFN: Bayesian Dynamic Causal Discovery using Generative Flow Networks. *Advances in Neural Information Processing Systems*, 2023.
- Philip Bachman and Doina Precup. Data Generation as Sequential Decision Making. *Advances in Neural Information Processing Systems*, 2015.
- Emmanuel Bengio, Moksh Jain, Maksym Korablyov, Doina Precup, and Yoshua Bengio. Flow Network based Generative Models for Non-Iterative Diverse Candidate Generation. *Advances in Neural Information Processing Systems*, 2021.
- Yoshua Bengio, Salem Lahlou, Tristan Deleu, Edward J Hu, Mo Tiwari, and Emmanuel Bengio. GFlowNet Foundations. *Journal of Machine Learning Research*, 2023.
- Kevin Black, Michael Janner, Yilun Du, Ilya Kostrikov, and Sergey Levine. Training Diffusion Models with Reinforcement Learning. *arXiv preprint*, 2023.
- Lars Buesing, Nicolas Heess, and Theophane Weber. Approximate Inference in Discrete Distributions with Monte Carlo Tree Search and Value Functions. In *International Conference on Artificial Intelligence and Statistics*. PMLR, 2020.
- Petros Christodoulou. Soft Actor-Critic for Discrete Action Settings. *arXiv preprint*, 2019.
- Tristan Deleu, António Góis, Chris Emezue, Mansi Rankawat, Simon Lacoste-Julien, Stefan Bauer, and Yoshua Bengio. Bayesian Structure Learning with Generative Flow Networks. *Uncertainty in Artificial Intelligence*, 2022.
- Tristan Deleu, Mizu Nishikawa-Toomey, Jithendaraa Subramanian, Nikolay Malkin, Laurent Charlin, and Yoshua Bengio. Joint Bayesian Inference of Graphical Structure and Parameters with a Single Generative Flow Network. *Advances in Neural Information Processing Systems*, 2023.
- Benjamin Eysenbach and Sergey Levine. Maximum Entropy RL (Provably) Solves Some Robust RL Problems. *International Conference on Learning Representations*, 2022.
- Jean-Pierre Falet, Hae Beom Lee, Nikolay Malkin, Chen Sun, Dragos Secrieru, Dinghui Zhang, Guillaume Lajoie, and Yoshua Bengio. Delta-AI: Local objectives for amortized inference in sparse graphical models. *International Conference on Learning Representations*, 2024.
- Ying Fan and Kangwook Lee. Optimizing ddpm sampling with shortcut fine-tuning. *International Conference on Machine Learning*, 2023.
- Leo Feng, Padideh Nouri, Aneri Muni, Yoshua Bengio, and Pierre-Luc Bacon. Designing Biological Sequences via Meta-Reinforcement Learning and Bayesian Optimization. *Workshop on Machine Learning in Structural Biology, NeurIPS*, 2022.
- Roy Fox, Ari Pakman, and Naftali Tishby. Taming the Noise in Reinforcement Learning via Soft Updates. *Uncertainty in Artificial Intelligence*, 2016.
- Dan Geiger and David Heckerman. Learning Gaussian Networks. *Uncertainty in Artificial Intelligence*, 1994.

- Matthieu Geist, Bruno Scherrer, and Olivier Pietquin. A Theory of Regularized Markov Decision Processes. *International Conference on Machine Learning*, 2019.
- Alan E. Gelfand and Adrian FM. Smith. Sampling-based approaches to calculating marginal densities. *Journal of the American statistical association*, 1990.
- Tuomas Haarnoja, Haoran Tang, Pieter Abbeel, and Sergey Levine. Reinforcement Learning with Deep Energy-Based Policies. *International Conference on Machine Learning*, 2017.
- Tuomas Haarnoja, Aurick Zhou, Pieter Abbeel, and Sergey Levine. Soft Actor-Critic: Off-Policy Maximum Entropy Deep Reinforcement Learning with a Stochastic Actor. In *International Conference in Machine Learning*, 2018a.
- Tuomas Haarnoja, Aurick Zhou, Kristian Hartikainen, George Tucker, Sehoon Ha, Jie Tan, Vikash Kumar, Henry Zhu, Abhishek Gupta, Pieter Abbeel, and Sergey Levine. Soft Actor-Critic Algorithms and Applications. *Arxiv preprint*, 2018b.
- W. Keith Hastings. Monte Carlo sampling methods using Markov chains and their applications. *Biometrika*, 1970.
- Alex Hernandez-Garcia, Nikita Saxena, Moksh Jain, Cheng-Hao Liu, and Yoshua Bengio. Multi-Fidelity Active Learning with GFlowNets. *arXiv preprint*, 2023.
- Edward J Hu, Nikolay Malkin, Moksh Jain, Katie E Everett, Alexandros Graikos, and Yoshua Bengio. GFlowNet-EM for Learning Compositional Latent Variable Models. *International Conference on Machine Learning*, 2023.
- Edward J Hu, Moksh Jain, Eric Elmoznino, Younesse Kaddar, Guillaume Lajoie, Yoshua Bengio, and Nikolay Malkin. Amortizing intractable inference in large language models. *International Conference on Learning Representations*, 2024.
- Moksh Jain, Emmanuel Bengio, Alex Hernandez-Garcia, Jarrid Rector-Brooks, Bonaventure F.P. Dossou, Chanakya Ekbote, Jie Fu, Tianyu Zhang, Micheal Kilgour, Dinghui Zhang, Lena Simine, Payel Das, and Yoshua Bengio. Biological Sequence Design with GFlowNets. *International Conference on Machine Learning*, 2022.
- Moksh Jain, Tristan Deleu, Jason Hartford, Cheng-Hao Liu, Alex Hernandez-Garcia, and Yoshua Bengio. GFlowNets for AI-Driven Scientific Discovery. *Digital Discovery*, 2023a.
- Moksh Jain, Sharath Chandra Raparthy, Alex Hernández-García, Jarrid Rector-Brooks, Yoshua Bengio, Santiago Miret, and Emmanuel Bengio. Multi-Objective GFlowNets. *International Conference on Machine Learning*, 2023b.
- Eric Jang, Shixiang Gu, and Ben Poole. Categorical Reparameterization with Gumbel-Softmax. In *International Conference on Learning Representations*, 2017.
- Marco Jiralerspong, Bilun Sun, Danilo Vucetic, Tianyu Zhang, Yoshua Bengio, Gauthier Gidel, and Nikolay Malkin. Expected flow networks in stochastic environments and two-player zero-sum games. *International Conference on Learning Representations*, 2024.
- Diederik P Kingma and Max Welling. Auto-Encoding Variational Bayes. *International Conference on Learning Representations*, 2014.
- Salem Lahlou, Tristan Deleu, Pablo Lemos, Dinghui Zhang, Alexandra Volokhova, Alex Hernández-García, Léna Néhale Ezzine, Yoshua Bengio, and Nikolay Malkin. A Theory of Continuous Generative Flow Networks. *International Conference on Machine Learning*, 2023.
- Sergey Levine. Reinforcement Learning and Control as Probabilistic Inference: Tutorial and Review. *arXiv preprint*, 2018.
- Yinchuan Li, Shuang Luo, Haozhi Wang, and Jianye Hao. CFlowNets: Continuous control with Generative Flow Networks. *International Conference on Learning Representations*, 2023.

- Kanika Madan, Jarrid Rector-Brooks, Maksym Korablyov, Emmanuel Bengio, Moksh Jain, Andrei Nica, Tom Bosc, Yoshua Bengio, and Nikolay Malkin. Learning GFlowNets from partial episodes for improved convergence and stability. *International Conference on Machine Learning*, 2023.
- Chris J. Maddison, Andriy Mnih, and Yee Whye Teh. The Concrete Distribution: A Continuous Relaxation of Discrete Random Variables. In *International Conference on Learning Representations*, 2017.
- Nikolay Malkin, Moksh Jain, Emmanuel Bengio, Chen Sun, and Yoshua Bengio. Trajectory balance: Improved credit assignment in GFlowNets. *Advances in Neural Information Processing Systems*, 2022.
- Nikolay Malkin, Salem Lahlou, Tristan Deleu, Xu Ji, Edward Hu, Katie Everett, Dinghuai Zhang, and Yoshua Bengio. GFlowNets and variational inference. *International Conference on Learning Representations*, 2023.
- Gonzalo Mena, David Belanger, Scott Linderman, and Jasper Snoek. Learning Latent Permutations with Gumbel-Sinkhorn Networks. In *International Conference on Learning Representations*, 2018.
- Mila AI4Science, Alex Hernandez-Garcia, Alexandre Duval, Alexandra Volokhova, Yoshua Bengio, Divya Sharma, Pierre Luc Carrier, Michał Koziarski, and Victor Schmidt. Crystal-GFN: sampling crystals with desirable properties and constraints. *arXiv preprint*, 2023.
- Shakir Mohamed, Mihaela Rosca, Michael Figurnov, and Andriy Mnih. Monte Carlo Gradient Estimation in Machine Learning. In *Journal of Machine Learning Research*, 2020.
- Sobhan Mohammadpour, Emmanuel Bengio, Emma Frejinger, and Pierre-Luc Bacon. Maximum entropy GFlowNets with soft Q-learning. *International Conference on Artificial Intelligence and Statistics (AISTATS)*, 2024.
- Ofir Nachum, Mohammad Norouzi, Kelvin Xu, and Dale Schuurmans. Bridging the Gap Between Value and Policy Based Reinforcement Learning. *Advances in Neural Information Processing Systems*, 2017.
- Andrew Y. Ng, Daishi Harada, and Stuart Russell. Policy Invariance Under Reward Transformations: Theory and Application to Reward Shaping. *International Conference on Machine Learning*, 1999.
- Mizu Nishikawa-Toomey, Tristan Deleu, Jithendaraa Subramanian, Yoshua Bengio, and Laurent Charlin. Bayesian learning of Causal Structure and Mechanisms with GFlowNets and Variational Bayes. *AAAI Workshop Graphs and More Complex Structures for Learning and Reasoning*, 2023.
- Ling Pan, Nikolay Malkin, Dinghuai Zhang, and Yoshua Bengio. Better Training of GFlowNets with Local Credit and Incomplete Trajectories. *International Conference on Machine Learning*, 2023a.
- Ling Pan, Dinghuai Zhang, Moksh Jain, Longbo Huang, and Yoshua Bengio. Stochastic Generative Flow Networks. *Uncertainty in Artificial Intelligence*, 2023b.
- Jarrid Rector-Brooks, Kanika Madan, Moksh Jain, Maksym Korablyov, Cheng-Hao Liu, Sarath Chandar, Nikolay Malkin, and Yoshua Bengio. Thompson sampling for improved exploration in GFlowNets. *ICML 2023 workshop on Structured Probabilistic Inference & Generative Modeling*, 2023.
- Danilo Rezende and Shakir Mohamed. Variational Inference with Normalizing Flows. In *International Conference on Machine Learning*, 2015.
- Danilo Jimenez Rezende, Shakir Mohamed, and Daan Wierstra. Stochastic Backpropagation and Approximate Inference in Deep Generative Models. In *International Conference on Machine Learning*, 2014.
- John Schulman, Xi Chen, and Pieter Abbeel. Equivalence Between Policy Gradients and Soft Q-Learning. *arXiv preprint*, 2017.

- Marcin Sendera, Minsu Kim, Sarthak Mittal, Pablo Lemos, Luca Scimeca, Jarrid Rector-Brooks, Alexandre Adam, Yoshua Bengio, and Nikolay Malkin. On diffusion models for amortized inference: Benchmarking and improving stochastic control and sampling. *arXiv preprint*, 2024.
- Max W Shen, Emmanuel Bengio, Ehsan Hajiramezani, Andreas Loukas, Kyunghyun Cho, and Tommaso Biancalani. Towards Understanding and Improving GFlowNet Training. *International Conference on Machine Learning*, 2023.
- Richard S Sutton and Andrew G Barto. *Reinforcement learning: An introduction*. MIT press, 2018.
- Daniil Tiapkin, Nikita Morozov, Alexey Naumov, and Dmitry Vetrov. Generative Flow Networks as Entropy-Regularized RL. *International Conference on Artificial Intelligence and Statistics (AISTATS)*, 2024.
- Nikhil Vemgal, Elaine Lau, and Doina Precup. An Empirical Study of the Effectiveness of Using a Replay Buffer on Mode Discovery in GFlowNets. *ICML 2023 workshop on Structured Probabilistic Inference & Generative Modeling*, 2023.
- Ziyu Wang, Tom Schaul, Matteo Hessel, Hado Hasselt, Marc Lanctot, and Nando Freitas. Dueling Network Architectures for Deep Reinforcement Learning. *International Conference on Machine Learning*, 2016.
- Theophane Weber, Nicolas Heess, Ali Eslami, John Schulman, David Wingate, and David Silver. Reinforced variational inference. *Advances in Neural Information Processing Systems (NIPS) Workshops*, 2015.
- Ronald J. Williams. Simple statistical gradient-following algorithms for connectionist reinforcement learning. In *Machine Learning*, 1992.
- Jiaxuan You, Bowen Liu, Zhitao Ying, Vijay Pande, and Jure Leskovec. Graph Convolutional Policy Network for Goal-Directed Molecular Graph Generation. *Advances in Neural Information Processing Systems*, 2018.
- David Zhang, Corrado Rainone, Markus Peschl, and Roberto Bondesan. Robust Scheduling with GFlowNets. *International Conference on Learning Representations*, 2023a.
- Dinghuai Zhang, Ricky T. Q. Chen, Nikolay Malkin, and Yoshua Bengio. Unifying Generative Models with GFlowNets and Beyond. *International Conference on Machine Learning – Beyond Bayes workshop*, 2022a.
- Dinghuai Zhang, Nikolay Malkin, Zhen Liu, Alexandra Volokhova, Aaron Courville, and Yoshua Bengio. Generative Flow Networks for Discrete Probabilistic Modeling. *International Conference on Machine Learning*, 2022b.
- Dinghuai Zhang, Hanjun Dai, Nikolay Malkin, Aaron Courville, Yoshua Bengio, and Ling Pan. Let the Flows Tell: Solving Graph Combinatorial Optimization Problems with GFlowNets. *Advances in Neural Information Processing Systems*, 2023b.
- Mingyang Zhou, Zichao Yan, Elliot Layne, Nikolay Malkin, Dinghuai Zhang, Moksh Jain, Mathieu Blanchette, and Yoshua Bengio. PhyloGFN: Phylogenetic inference with generative flow networks. *International Conference on Machine Learning*, 2024.
- Brian D Ziebart. *Modeling Purposeful Adaptive Behavior with the Principle of Maximum Causal Entropy*. Carnegie Mellon University, 2010.
- Brian D Ziebart, Andrew L Maas, J Andrew Bagnell, Anind K Dey, et al. Maximum Entropy Inverse Reinforcement Learning. *AAAI Conference on Artificial Intelligence*, 2008.
- Heiko Zimmermann, Fredrik Lindsten, Jan-Willem van de Meent, and Christian A. Naesseth. A Variational Perspective on Generative Flow Networks. *Transactions of Machine Learning Research*, 2022.

Appendix

A Reward correction

Theorem 3.1 (Gen. of [Tiapkin et al., 2024](#); Theorem 1). *Let $P_B(\cdot | s')$ be an arbitrary backward transition probability (i.e., a distribution over the parents of $s' \neq s_0$ in \mathcal{G}). Let $r(s, s')$ be the reward function of the MDP corrected with P_B , satisfying for any trajectory $\tau = (s_0, s_1, \dots, s_T, s_f)$:*

$$\sum_{t=0}^T r(s_t, s_{t+1}) = -\mathcal{E}(s_T) + \alpha \sum_{t=0}^{T-1} \log P_B(s_t | s_{t+1}), \quad (8)$$

where we used the convention $s_{T+1} = s_f$. Then the terminating state distribution associated with the optimal policy π_{MaxEnt}^* solution of (3) satisfies $\pi^*(x) \propto \exp(-\mathcal{E}(x)/\alpha)$.

Proof. Recall from [Ziebart \(2010\)](#); [Haarnoja et al. \(2017\)](#) that the optimal policy maximizing (3) is

$$\pi_{\text{MaxEnt}}^*(s' | s) = \exp\left(\frac{1}{\alpha}(Q_{\text{soft}}^*(s, s') - V_{\text{soft}}^*(s))\right), \quad (17)$$

where the soft value functions Q_{soft}^* and V_{soft}^* satisfy the soft Bellman optimality equations, adapted to our deterministic soft MDP:

$$Q_{\text{soft}}^*(s, s') = r(s, s') + V_{\text{soft}}^*(s') \quad (18)$$

$$V_{\text{soft}}^*(s') = \alpha \log \sum_{s'' \in \text{Ch}(s')} \exp\left(\frac{1}{\alpha} Q_{\text{soft}}^*(s', s'')\right). \quad (19)$$

By definition of the terminating state distribution associated with π_{MaxEnt}^* in (5), for any terminating state $x \in \mathcal{X}$:

$$\pi^*(x) = \sum_{\tau: s_0 \rightsquigarrow x} \prod_{t=0}^{T_\tau} \pi_{\text{MaxEnt}}^*(s_{t+1} | s_t) \quad (20)$$

$$= \sum_{\tau: s_0 \rightsquigarrow x} \exp\left[\frac{1}{\alpha} \sum_{t=0}^{T_\tau} (Q_{\text{soft}}^*(s_t, s_{t+1}) - V_{\text{soft}}^*(s_t))\right] \quad (21)$$

$$= \sum_{\tau: s_0 \rightsquigarrow x} \exp\left[\frac{1}{\alpha} \sum_{t=0}^{T_\tau} (r(s_t, s_{t+1}) + V_{\text{soft}}^*(s_{t+1}) - V_{\text{soft}}^*(s_t))\right] \quad (22)$$

$$= \sum_{\tau: s_0 \rightsquigarrow x} \exp\left[\frac{1}{\alpha} \left(\sum_{t=0}^{T_\tau} r(s_t, s_{t+1}) + \underbrace{V_{\text{soft}}^*(s_f) - V_{\text{soft}}^*(s_0)}_{=0}\right)\right] \quad (23)$$

$$= \sum_{\tau: s_0 \rightsquigarrow x} \exp\left[\frac{1}{\alpha} \left(-\mathcal{E}(x) + \alpha \sum_{t=0}^{T_\tau-1} \log P_B(s_t | s_{t+1}) - V_{\text{soft}}^*(s_0)\right)\right] \quad (24)$$

$$= \exp\left[\frac{1}{\alpha}(-\mathcal{E}(x) - V_{\text{soft}}^*(s_0))\right] \underbrace{\sum_{\tau: s_0 \rightsquigarrow x} \prod_{t=0}^{T_\tau-1} P_B(s_t | s_{t+1})}_{=1} \quad (25)$$

$$= \frac{\exp(-\mathcal{E}(x)/\alpha)}{\exp(V_{\text{soft}}^*(s_0)/\alpha)} \propto \exp(-\mathcal{E}(x)/\alpha), \quad (26)$$

where we used in (25) the fact that P_B induces a probability distribution over the complete trajectories leading to any terminating state x ; see for example ([Bengio et al., 2023](#), Lemma 5) for a proof of this result. \square

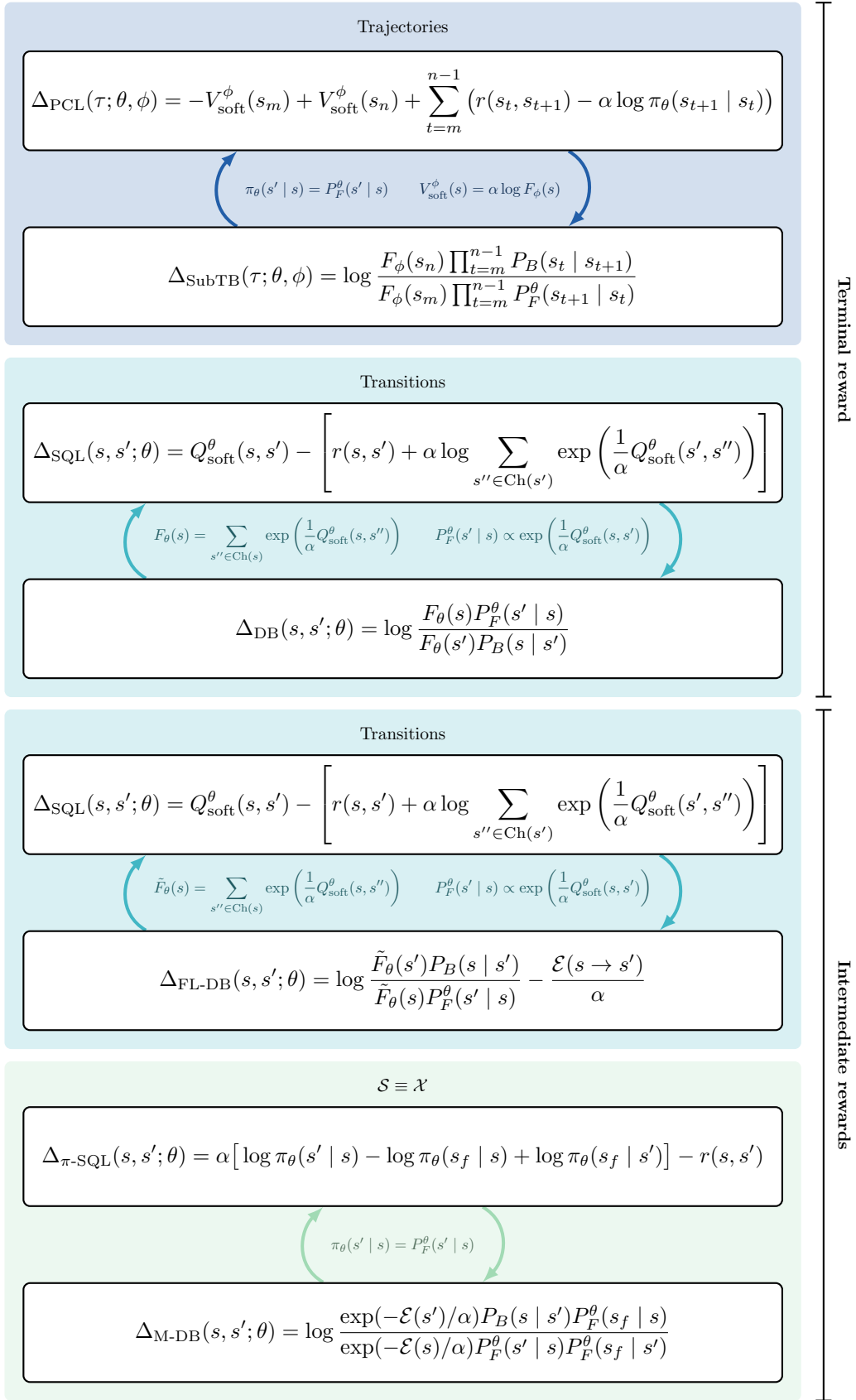


Figure 6: Summary of the equivalences between the MaxEnt RL (top, in each box) and GFlowNet (bottom, in each box) objectives, using the classification of Figure 2. All objectives can be written as $\mathcal{L}(\cdot) = \frac{1}{2} \mathbb{E}_{\pi_b} [\Delta^2(\cdot)]$, where π_b is a distribution over appropriate quantities (*i.e.*, trajectories, or transitions). The *terminal reward* setting corresponds to $r(s_t, s_{t+1}) = \alpha \log P_B(s_t | s_{t+1})$ & $r(s_T, s_f) = -\mathcal{E}(s_T)$ (Section 3.2), whereas the *intermediate rewards* setting corresponds to $r(s_t, s_{t+1}) = -\mathcal{E}(s_t \rightarrow s_{t+1}) + \alpha \log P_B(s_t | s_{t+1})$ (with $\mathcal{E}(s_t \rightarrow s_{t+1}) = \mathcal{E}(s_{t+1}) - \mathcal{E}(s_t)$ if $S \equiv \mathcal{X}$, Section 3.3) & $r(s_T, s_f) = 0$ (Appendix B.4)

Table 1: Summary of the equivalence results and their proofs in Appendix B.

MaxEnt RL	GFlowNet	Proposition	Proof
PCL (Nachum et al., 2017)	SubTB (Madan et al., 2023)	Proposition 3.2	App. B.1
SQL (Haarnoja et al., 2017)	DB (Bengio et al., 2023)	Corollary B.1	App. B.2
SQL* (Haarnoja et al., 2017)	FL-DB (Pan et al., 2023a)	Proposition B.3	App. B.4
π -SQL* (Section 3.3)	M-DB (Deleu et al., 2022)	Proposition 3.3	App. B.3

B Equivalences between MaxEnt RL & GFlowNet objectives

In this section, we detail all of our new results establishing equivalences between MaxEnt RL and GFlowNet objectives, along with their proofs. We summarize the results with links to the propositions and proofs in Table 1. All the objectives considered in this paper take the form of an (expected) least-square $\mathcal{L}(\cdot) = \frac{1}{2} \mathbb{E}_{\pi_b} [\Delta^2(\cdot)]$, where $\Delta(\cdot)$ is a residual term that is algorithm-dependent, and π_b is a distribution over appropriate quantities (*i.e.*, trajectories, or transitions); see Section 3.2 for an example with the PCL & SubTB objectives. In this section, we will work exclusively with residuals for simplicity, instead of the objectives themselves. We summarize the different residuals and their correspondences in Figure 6.

B.1 Equivalence between PCL & SubTB

Proposition 3.2. *The Subtrajectory Balance objective (GFlowNet; Madan et al., 2023) is proportional to the Path Consistency Learning objective (MaxEnt RL; Nachum et al., 2017) on the soft MDP with the reward function defined in (9), in the sense that $\mathcal{L}_{\text{PCL}}(\theta, \phi) = \alpha^2 \mathcal{L}_{\text{SubTB}}(\theta, \phi)$, with the following correspondence*

$$\pi_\theta(s' | s) = P_F^\theta(s' | s) \quad V_{\text{soft}}^\phi(s) = \alpha \log F_\phi(s). \quad (12)$$

Proof. Let $\tau = (s_m, s_{m+1}, \dots, s_n)$ be a subtrajectory, where s_n may be the terminal state s_f . We first recall the definitions of the Path Consistency Learning (PCL; Nachum et al., 2017) and the Subtrajectory Balance (SubTB; Madan et al., 2023; Malkin et al., 2022) objectives. On the one hand, the PCL objective encourages the consistency between a policy π_θ parametrized by θ and a value function V_{soft}^ϕ parametrized by ϕ :

$$\Delta_{\text{PCL}}(\tau; \theta, \phi) = -V_{\text{soft}}^\phi(s_m) + V_{\text{soft}}^\phi(s_n) + \sum_{t=m}^{n-1} (r(s_t, s_{t+1}) - \alpha \log \pi_\theta(s_{t+1} | s_t)). \quad (27)$$

On the other hand, the SubTB objective also encourages some form of consistency, but this time between a policy (forward transition probability) P_F^θ parametrized by θ and a flow function F_ϕ parametrized by ϕ . We will give the form of its residual further down, as it depends on the trajectory τ . Finally, recall that the reward function of the soft MDP is defined by (9), in order to satisfy the reward correction necessary for the application of Theorem 3.1, following the same decomposition as in (Tiapkin et al., 2024)

$$r(s_t, s_{t+1}) = \alpha \log P_B(s_t | s_{t+1}) \quad r(s_T, s_f) = -\mathcal{E}(s_T). \quad (28)$$

In order to show the equivalence between \mathcal{L}_{PCL} and $\mathcal{L}_{\text{SubTB}}$, we only need to show equivalence of their corresponding residuals, by replacing the reward by its definition above. We will use the correspondence in (12) between the policy/value function of PCL and the policy/flow function of SubTB. We consider two cases:

- If $s_n \neq s_f$ is not the terminal state, then the residual for SubTB can be written as

$$\Delta_{\text{SubTB}}(\tau; \theta, \phi) = \log \frac{F_\phi(s_n) \prod_{t=m}^{n-1} P_B(s_t | s_{t+1})}{F_\phi(s_m) \prod_{t=m}^{n-1} P_F^\theta(s_{t+1} | s_t)}, \quad (29)$$

where P_B is a backward transition probability. Although it is in general possible to learn P_B (Malkin et al., 2022), we will consider it fixed here. Substituting (12) into the residual Δ_{PCL} :

$$\begin{aligned}\Delta_{\text{PCL}}(\tau; \theta, \phi) &= -V_{\text{soft}}^\phi(s_m) + V_{\text{soft}}^\phi(s_n) + \alpha \sum_{t=m}^{n-1} (\log P_B(s_t | s_{t+1}) - \log \pi_\theta(s_{t+1} | s_t)) \\ &= -\alpha \log F_\phi(s_m) + \alpha \log F_\phi(s_n) + \alpha \sum_{t=m}^{n-1} (\log P_B(s_t | s_{t+1}) - \log P_F^\theta(s_{t+1} | s_t)) \\ &= \alpha \log \frac{F_\phi(s_n) \prod_{t=m}^{n-1} P_B(s_t | s_{t+1})}{F_\phi(s_m) \prod_{t=m}^{n-1} P_F^\theta(s_{t+1} | s_t)} = \alpha \Delta_{\text{SubTB}}(\tau; \theta, \phi).\end{aligned}\quad (30)$$

- If $s_n = s_f$, then the residual Δ_{SubTB} appearing in the Subtrajectory Balance objective must be written as

$$\Delta_{\text{SubTB}}(\tau; \theta, \phi) = \log \frac{\exp(-\mathcal{E}(s_{n-1})/\alpha) \prod_{t=m}^{n-2} P_B(s_t | s_{t+1})}{F_\phi(s_m) \prod_{t=m}^{n-1} P_F^\theta(s_{t+1} | s_t)}, \quad (31)$$

since the boundary conditions must also be enforced (Malkin et al., 2022). Moreover, by definition of the value function, we can also enforce that $V_{\text{soft}}^\phi(s_f) = 0$. Therefore

$$\begin{aligned}\Delta_{\text{PCL}}(\tau; \theta, \phi) &= -V_{\text{soft}}^\phi(s_m) + V_{\text{soft}}^\phi(s_f) - (\mathcal{E}(s_{n-1}) + \alpha \log \pi_\theta(s_f | s_{n-1})) \\ &\quad + \alpha \sum_{t=m}^{n-2} (\log P_B(s_t | s_{t+1}) - \log \pi_\theta(s_{t+1} | s_t))\end{aligned}\quad (32)$$

$$\begin{aligned}&= -\alpha \log F_\phi(s_m) - \mathcal{E}(s_{n-1}) - \alpha \log P_F^\theta(s_f | s_{n-1}) \\ &\quad + \alpha \sum_{t=m}^{n-2} (\log P_B(s_t | s_{t+1}) - \log P_F^\theta(s_{t+1} | s_t))\end{aligned}\quad (33)$$

$$= \alpha \Delta_{\text{SubTB}}(\tau; \theta, \phi). \quad (34)$$

Note that the Trajectory Balance objective, operating only at the level of complete trajectories (Malkin et al., 2022), corresponds to this case where $s_m = s_0$ is the initial state.

This concludes the proof, showing that $\mathcal{L}_{\text{PCL}}(\theta, \phi) = \alpha^2 \mathcal{L}_{\text{SubTB}}(\theta, \phi)$. \square

B.2 Equivalence between SQL & DB

The following result establishing the equivalence between the objectives in SQL and DB can be seen as a direct consequence of Proposition 3.2, under the Unified PCL perspective of Nachum et al. (2017). We state and prove this as a standalone result for completeness.

Corollary B.1. *The Detailed Balance objective (GFlowNet; Bengio et al., 2023) is proportional to the Soft Q-Learning objective (MaxEnt RL; Haarnoja et al., 2017) on the soft MDP with the reward function defined in (9), in the sense that $\mathcal{L}_{\text{SQL}}(\theta) = \alpha^2 \mathcal{L}_{\text{DB}}(\theta)$, with the following correspondence*

$$F_\theta(s) = \sum_{s'' \in \text{Ch}(s)} \exp\left(\frac{1}{\alpha} Q_{\text{soft}}^\theta(s, s'')\right) \quad P_F^\theta(s' | s) \propto \exp\left(\frac{1}{\alpha} Q_{\text{soft}}^\theta(s, s')\right). \quad (35)$$

Proof. Let $s \rightarrow s'$ be a transition in the soft MDP, where s' may be the terminal state. Recall that the residual in the SQL objective depends on a Q-function Q_{soft}^θ parametrized by θ :

$$\Delta_{\text{SQL}}(s, s'; \theta) = Q_{\text{soft}}^\theta(s, s') - (r(s, s') + V_{\text{soft}}^\theta(s')), \quad (36)$$

$$\text{where } V_{\text{soft}}^\theta(s') \triangleq \alpha \log \sum_{s'' \in \text{Ch}(s')} \exp\left(\frac{1}{\alpha} Q_{\text{soft}}^\theta(s', s'')\right). \quad (37)$$

In the case where $s' = s_f$ is the terminal state, then $V_{\text{soft}}^\theta(s') = 0$. On the other hand, the exact form of the residual in the DB objective will be given further down, but always depends on a forward transition probability P_F^θ and a state flow function F_θ , which we assume are sharing parameters θ . We consider two cases:

- If $s' \neq s_f$ is not the terminal state, then the residual in the DB objective is given by

$$\Delta_{\text{DB}}(s, s'; \theta) = \log \frac{F_\theta(s)P_F^\theta(s' | s)}{F_\theta(s')P_B(s | s')}. \quad (38)$$

With the definition of the reward function in (9), we know that $r(s, s') = \alpha \log P_B(s | s')$. We can therefore show that the residuals of SQL and DB are proportional to one-another:

$$\Delta_{\text{SQL}}(s, s'; \theta) = Q_{\text{soft}}^\theta(s, s') - r(s, s') - \alpha \log \sum_{s'' \in \text{Ch}(s')} \exp \left[\frac{1}{\alpha} Q_{\text{soft}}^\theta(s', s'') \right] \quad (39)$$

$$= Q_{\text{soft}}^\theta(s, s') - \alpha \log P_B(s | s') - \alpha \log \sum_{s'' \in \text{Ch}(s')} \exp \left[\frac{1}{\alpha} Q_{\text{soft}}^\theta(s', s'') \right] \quad (40)$$

$$= \alpha \log \left(\exp \left(\frac{1}{\alpha} Q_{\text{soft}}^\theta(s, s') \right) \right) - \alpha \log P_B(s | s') - \alpha \log \sum_{s'' \in \text{Ch}(s')} \exp \left[\frac{1}{\alpha} Q_{\text{soft}}^\theta(s', s'') \right] \\ - \alpha \log \sum_{s'' \in \text{Ch}(s)} \exp \left[\frac{1}{\alpha} Q_{\text{soft}}^\theta(s, s'') \right] + \alpha \log \sum_{s'' \in \text{Ch}(s)} \exp \left[\frac{1}{\alpha} Q_{\text{soft}}^\theta(s, s'') \right] \quad (41)$$

$$= \alpha \left[\log P_F^\theta(s' | s) + \log F_\theta(s) - \log P_B(s | s') - \log F_\theta(s') \right] \quad (42)$$

$$= \alpha \Delta_{\text{DB}}(s, s'; \theta), \quad (43)$$

where we used the following correspondence between Q_{soft}^θ , P_F^θ , and F_θ :

$$F_\theta(s') = \sum_{s \in \text{Pa}(s')} \exp \left(\frac{1}{\alpha} Q_{\text{soft}}^\theta(s, s') \right) \quad P_F^\theta(s' | s) \propto \exp \left(\frac{1}{\alpha} Q_{\text{soft}}^\theta(s, s') \right). \quad (44)$$

- If $s' = s_f$ is the terminal state, then the residual in the DB objective is

$$\Delta_{\text{DB}}(s, s_f; \theta) = \log \frac{F_\theta(s)P_F^\theta(s_f | s)}{\exp(-\mathcal{E}(s)/\alpha)}. \quad (45)$$

Again with our definition of the reward function of the soft MDP in (9), we know that the reward of the terminating transition is $r(s, s_f) = -\mathcal{E}(s)$. We can therefore also show the relation between the two residuals in this case:

$$\Delta_{\text{SQL}}(s, s_f; \theta) = Q_{\text{soft}}^\theta(s, s_f) - r(s, s_f) \quad (46)$$

$$= Q_{\text{soft}}^\theta(s, s_f) + \mathcal{E}(s) \quad (47)$$

$$= \alpha \log \left(\exp \left(\frac{1}{\alpha} Q_{\text{soft}}^\theta(s, s_f) \right) \right) + \mathcal{E}(s) \quad (48)$$

$$- \alpha \log \sum_{s'' \in \text{Ch}(s)} \exp \left[\frac{1}{\alpha} Q_{\text{soft}}^\theta(s, s'') \right] + \alpha \log \sum_{s'' \in \text{Ch}(s)} \exp \left[\frac{1}{\alpha} Q_{\text{soft}}^\theta(s, s'') \right]$$

$$= \alpha \left[\log P_F^\theta(s_f | s) + \log F_\theta(s) + \frac{\mathcal{E}(s)}{\alpha} \right] \quad (49)$$

$$= \alpha \Delta_{\text{DB}}(s, s_f; \theta), \quad (50)$$

where we used the same correspondence between Q_{soft}^θ , P_F^θ , and F_θ as above.

This concludes the proof, showing that $\mathcal{L}_{\text{SQL}}(\theta) = \alpha^2 \mathcal{L}_{\text{DB}}(\theta)$. \square

Note that [Tiapkin et al. \(2024\)](#) established a similar connection between SQL and DB through a dueling architecture perspective ([Wang et al., 2016](#)), where the Q-function must be decomposed as (with notation adapted to this paper)

$$Q^\theta(s, s') = V^\theta(s) + A^\theta(s, s') - \log \sum_{s'' \in \text{Ch}(s)} \exp(A^\theta(s, s'')), \quad (51)$$

where $A^\theta(s, s')$ is an advantage function. The connection they establish is then between V^θ and the state flow on the one hand, and A^θ and the policy on the other hand, via

$$\log F_\theta(s) = V^\theta(s) = \log \sum_{s'' \in \text{Ch}(s)} \exp(Q^\theta(s, s'')) \quad (52)$$

$$\log P_F^\theta(s' | s) = A^\theta(s, s') - \log \sum_{s'' \in \text{Ch}(s)} \exp(A^\theta(s, s'')). \quad (53)$$

This differs from our result in that [Corollary B.1](#) does not explicitly require a separate advantage function. However, we note that both results are effectively equivalent to one another, since (52) directly corresponds to (35) in [Corollary B.1](#) (with $\alpha = 1$), and starting from (53):

$$\log P_F^\theta(s' | s) = A^\theta(s, s') - \log \sum_{s'' \in \text{Ch}(s)} \exp(A^\theta(s, s'')) \quad (54)$$

$$\begin{aligned} &= \left[Q^\theta(s, s') - V^\theta(s) + \log \sum_{s'' \in \text{Ch}(s)} \exp(A^\theta(s, s'')) \right] - \log \sum_{s'' \in \text{Ch}(s)} \exp(A^\theta(s, s'')) \\ &= Q^\theta(s, s') - V^\theta(s) = Q^\theta(s, s') - \log \sum_{s'' \in \text{Ch}(s)} \exp(Q^\theta(s, s'')), \end{aligned} \quad (55)$$

which also corresponds to (35) in [Corollary B.1](#). The connection through a dueling architecture is closer to DB when the policy and the state flow network are parametrized by two separate networks.

B.3 Equivalence between π -SQL and Modified DB

Proposition B.2. *Assume that all the states of the soft MDP are terminating (i.e., connected to the terminal state s_f), and such that for all $s \in \mathcal{S}$, the reward function satisfies $r(s, s_f) = 0$. Then the objective of Soft Q-Learning ([Haarnoja et al., 2017](#)) can be written as a function of a policy π_θ parametrized by θ . This objective is given by $\mathcal{L}_{\pi\text{-SQL}}(\theta) = \frac{1}{2} \mathbb{E}_{\pi_b} [\Delta_{\pi\text{-SQL}}^2(s, s'; \theta)]$, where π_b is an arbitrary policy over transitions $s \rightarrow s'$ such that $s' \neq s_f$, and*

$$\Delta_{\pi\text{-SQL}}(s, s'; \theta) = \alpha \left[\log \pi_\theta(s' | s) - \log \pi_\theta(s_f | s) + \log \pi_\theta(s_f | s') \right] - r(s, s'). \quad (56)$$

Proof. Recall that the objective of Soft Q-Learning can be written in terms of a Q-function Q_{soft}^θ parametrized by θ as $\mathcal{L}_{\text{SQL}}(\theta) = \frac{1}{2} \mathbb{E}_{\pi_b} [\Delta_{\text{SQL}}^2(s, s'; \theta)]$, with

$$\Delta_{\text{SQL}}(s, s'; \theta) = Q_{\text{soft}}^\theta(s, s') - (r(s, s') + V_{\text{soft}}^\theta(s')), \quad (57)$$

$$\text{where } V_{\text{soft}}^\theta(s') \triangleq \alpha \log \sum_{s'' \in \text{Ch}(s')} \exp \left[\frac{1}{\alpha} Q_{\text{soft}}^\theta(s', s'') \right]. \quad (58)$$

Since we assume that $r(s, s_f) = 0$, we can enforce the fact that $Q_{\text{soft}}^\theta(s, s_f) = 0$ in our parametrization of the Q-function. If we define a policy π_θ as

$$\pi_\theta(s' | s) \triangleq \exp \left[\frac{1}{\alpha} (Q_{\text{soft}}^\theta(s, s') - V_{\text{soft}}^\theta(s)) \right], \quad (59)$$

then we have in particular $\pi_\theta(s_f | s) = \exp(-V_{\text{soft}}^\theta(s)/\alpha)$, based on our observation above. Moreover, we can write the different in value functions appearing in (57) as

$$Q_{\text{soft}}^\theta(s, s') - V_{\text{soft}}^\theta(s') = Q_{\text{soft}}^\theta(s, s') - V_{\text{soft}}^\theta(s) + V_{\text{soft}}^\theta(s) - V_{\text{soft}}^\theta(s') \quad (60)$$

$$= \alpha \left[\log \pi_\theta(s' | s) - \log \pi_\theta(s_f | s) + \log \pi_\theta(s_f | s') \right] \quad (61)$$

which concludes the proof. \square

Proposition 3.3. *Suppose that all the states of the soft MDP are terminating $\mathcal{S} \equiv \mathcal{X}$. The Modified Detailed Balance objective (GFlowNet; [Deleu et al., 2022](#)) is proportional to the Soft Q-Learning objective with a policy parametrization (MaxEnt RL; π -SQL) on the soft MDP with the reward function defined in (13), in the sense that $\mathcal{L}_{\pi\text{-SQL}}(\theta) = \alpha^2 \mathcal{L}_{\text{M-DB}}(\theta)$, with $\pi_\theta(s' | s) = P_F^\theta(s' | s)$.*

Proof. Let $s \rightarrow s'$ be a transition in the soft MDP. In order to show the equivalence between $\mathcal{L}_{\pi\text{-SQL}}$ and $\mathcal{L}_{\text{M-DB}}$, it is sufficient to show the equivalence between their corresponding residuals (14) and (15). Recall that the reward function in (13) is defined by

$$r(s_t, s_{t+1}) = \mathcal{E}(s_t) - \mathcal{E}(s_{t+1}) + \alpha \log P_B(s_t | s_{t+1}) \quad r(s_T, s_f) = 0. \quad (62)$$

Replacing the reward in the residual $\Delta_{\pi\text{-SQL}}$, we get

$$\begin{aligned} \Delta_{\pi\text{-SQL}}(s, s'; \theta) &= \alpha [\log \pi_\theta(s' | s) - \log \pi_\theta(s_f | s) + \log \pi_\theta(s_f | s')] - r(s, s') \\ &= \alpha [\log \pi_\theta(s' | s) - \log \pi_\theta(s_f | s) + \log \pi_\theta(s_f | s')] - [\mathcal{E}(s) - \mathcal{E}(s') + \alpha \log P_B(s | s')] \\ &= \alpha \left[-\frac{\mathcal{E}(s)}{\alpha} + \log \pi_\theta(s' | s) + \log \pi_\theta(s_f | s') + \frac{\mathcal{E}(s')}{\alpha} - \log P_B(s | s') - \log \pi_\theta(s_f | s) \right] \\ &= \alpha \left[-\frac{\mathcal{E}(s)}{\alpha} + \log P_F^\theta(s' | s) + \log P_F^\theta(s_f | s') + \frac{\mathcal{E}(s')}{\alpha} - \log P_B(s | s') - \log P_F^\theta(s_f | s) \right] \\ &= -\alpha \log \frac{\exp(-\mathcal{E}(s')/\alpha) P_B(s | s') P_F^\theta(s_f | s)}{\exp(-\mathcal{E}(s)/\alpha) P_F^\theta(s' | s) P_F^\theta(s_f | s')} = -\alpha \Delta_{\text{M-DB}}(s, s'; \theta) \end{aligned}$$

This concludes the proof, showing that $\mathcal{L}_{\pi\text{-SQL}}(\theta) = \alpha^2 \mathcal{L}_{\text{M-DB}}(\theta)$. \square

B.4 Equivalence between SQL and Forward-Looking DB

We will now generalize the result of Proposition 3.3 to the case where $\mathcal{X} \neq \mathcal{S}$, but where intermediate rewards are still available along the trajectory. We will assume that for any complete trajectory $\tau = (s_0, s_1, \dots, s_T, s_f)$, the energy function at s_T can be decomposed into a sum of intermediate rewards (Pan et al., 2023a)

$$\mathcal{E}(s_T) = \sum_{t=0}^{T-1} \mathcal{E}(s_t \rightarrow s_{t+1}), \quad (63)$$

where we overload the notation \mathcal{E} for simplicity. In that case, we can define the corrected reward as follows in order to satisfy the conditions of Theorem 3.1

$$r(s_t, s_{t+1}) = -\mathcal{E}(s_t \rightarrow s_{t+1}) + \alpha \log P_B(s_t | s_{t+1}) \quad r(s_T, s_f) = 0. \quad (64)$$

This type of reward shaping is similar to the one introduced in Section 3.3. The Forward-Looking Detailed Balance loss (FL-DB; Pan et al., 2023a) is defined similarly to DB, with the exception that the flow function corresponds to the unknown offset relative to $\mathcal{E}(s_t \rightarrow s_{t+1})$, which is known and therefore does not need to be learned. For some transition $s \rightarrow s'$ such that $s' \neq s_f$, the corresponding residual can be written as

$$\Delta_{\text{FL-DB}}(s, s'; \theta) = \log \frac{\tilde{F}_\theta(s') P_B(s | s')}{\tilde{F}_\theta(s) P_F^\theta(s' | s)} - \frac{\mathcal{E}(s \rightarrow s')}{\alpha}, \quad (65)$$

where P_F^θ is the policy (forward transition probability), and \tilde{F}_θ is an offset state-flow function, parametrized by θ . Note that with FL-DB, there is no longer an explicit residual for the boundary condition, unlike in DB, since this is captured through (65) already. The following proposition establishes an equivalence between SQL and FL-DB, similar to Corollary B.1 & Proposition 3.3.

Proposition B.3. *The Forward-Looking Detailed Balance objective (GFlowNet; Pan et al., 2023a) is proportional to the Soft Q-Learning objective (MaxEnt RL; Haarnoja et al., 2017) on the soft MDP with the reward function defined in (64), in the sense that $\mathcal{L}_{\text{SQL}}(\theta) = \alpha^2 \mathcal{L}_{\text{FL-DB}}(\theta)$, with the following correspondence*

$$\tilde{F}_\theta(s) = \sum_{s'' \in \text{Ch}(s)} \exp\left(\frac{1}{\alpha} Q_{\text{soft}}^\theta(s, s'')\right) \quad P_F^\theta(s' | s) \propto \exp\left(\frac{1}{\alpha} Q_{\text{soft}}^\theta(s, s')\right). \quad (66)$$

Proof. The proof is similar to the one in Appendix B.2. Let $s \rightarrow s'$ be a transition in the soft MDP, where $s' \neq s_f$. Recall that the residual in the SQL objective is

$$\Delta_{\text{SQL}}(s, s'; \theta) = Q_{\text{soft}}^\theta(s, s') - (r(s, s') + V_{\text{soft}}^\theta(s')), \quad (67)$$

$$\text{where } V_{\text{soft}}^\theta(s') \triangleq \alpha \log \sum_{s'' \in \text{Ch}(s')} \exp\left(\frac{1}{\alpha} Q_{\text{soft}}^\theta(s', s'')\right). \quad (68)$$

With our choice of reward function in (64), we know that $r(s, s') = -\mathcal{E}(s \rightarrow s') + \alpha \log P_B(s | s')$. We can therefore show that the residuals of SQL and FL-DB are proportional to one-another:

$$\Delta_{\text{SQL}}(s, s'; \theta) = Q_{\text{soft}}^\theta(s, s') - (r(s, s') + V_{\text{soft}}^\theta(s')) \quad (69)$$

$$= Q_{\text{soft}}^\theta(s, s') + \mathcal{E}(s \rightarrow s') - \alpha \log P_B(s | s') - \alpha \log \sum_{s'' \in \text{Ch}(s')} \exp\left(\frac{1}{\alpha} Q_{\text{soft}}^\theta(s', s'')\right) \quad (70)$$

$$= Q_{\text{soft}}^\theta(s, s') - \alpha \log \sum_{s'' \in \text{Ch}(s)} \exp\left(\frac{1}{\alpha} Q_{\text{soft}}^\theta(s, s'')\right) + \mathcal{E}(s \rightarrow s') - \alpha \log P_B(s | s') \\ + \alpha \log \sum_{s'' \in \text{Ch}(s)} \exp\left(\frac{1}{\alpha} Q_{\text{soft}}^\theta(s, s'')\right) - \alpha \log \sum_{s'' \in \text{Ch}(s')} \exp\left(\frac{1}{\alpha} Q_{\text{soft}}^\theta(s', s'')\right) \quad (71)$$

$$= \alpha \left[\log P_F^\theta(s' | s) - \log P_B(s | s') + \log \tilde{F}_\theta(s) - \log \tilde{F}_\theta(s') + \frac{\mathcal{E}(s \rightarrow s')}{\alpha} \right] \quad (72)$$

$$= -\alpha \Delta_{\text{FL-DB}}(s, s'; \theta). \quad (73)$$

Where we used the correspondence between \tilde{F}_θ , P_F^θ , and Q_{soft}^θ from (66). This concludes the proof, showing that $\mathcal{L}_{\text{SQL}}(\theta) = \alpha^2 \mathcal{L}_{\text{FL-DB}}(\theta)$. \square

Interestingly, the correspondence in (66) between state flows and policy on the one hand (GFlowNet) and the Q-function on the other hand (MaxEnt RL) is exactly the same as the one in Corollary B.1.

C Experimental details

For all algorithms and all environments (unless stated otherwise), we kept the same exploration schedule, frequency of update of the target network (if applicable), and replay buffer, in order to avoid attributing favorable performance to any of those components. Exploration was done using a naive ε -sampling scheme, where actions were sampled from the current policy with probability $1 - \varepsilon$, and uniformly at random with probability ε . All algorithms were trained over 100k iterations, and ε was decreasing over the first 50k from $\varepsilon = 1$ to $\varepsilon = 0.1$. All algorithms use a target network, except TB/PCL, and the target network was updated every 1000 iterations. We used a simple circular buffer with 100k capacity for all algorithms (TB/PCL using buffer of trajectories, as opposed to a buffer of transitions). Hyperparameter search was conducted for all environments over the learning rate alone of all the networks, using a simple grid search.

C.1 Probabilistic inference over discrete factor graphs

Given a factor graph with a fixed structure, over d random variables (V_1, \dots, V_d) , the objective is to sample a complete assignment \mathbf{v} of these variables from the Gibbs distribution $P(\mathbf{v}) \propto \exp(-\mathcal{E}(\mathbf{v}))$, where the energy function is defined by

$$\mathcal{E}(v_1, \dots, v_d) = - \sum_{m=1}^M \psi_m(\mathbf{v}_{[m]}), \quad (74)$$

where ψ_m is the m th factor in the factor graph, and $\mathbf{v}_{[m]}$ represents the values of the variables that are part of this factor. The factors ψ_m are fixed, and randomly generated using the same process as Buesing et al. (2020). Each variable V_i is assumed to be discrete and can take one of K possible values. Overall, this means that the number of elements in the sample space is K^d .

A state of the soft MDP is a (possibly partial) assignment of the values, e.g., $(0, \cdot, 1, 0, \cdot, \cdot)$, where \cdot represents a variable which has not been assigned a value yet. The initial state $s_0 = (\cdot, \cdot, \dots, \cdot)$ is the state where no variable has an assigned value. An action consists in picking one variable that has not value (with a \cdot), and assigning it one of K values. The process terminates when all the variables have been assigned a value, meaning that all the complete trajectories have length d . This differs from the MDP of Buesing et al. (2020), since they were assigning the values of the variables in a fixed order determined ahead of time, making the MDP having a tree structure.

Table 2: Statistics of the datasets used in the phylogenetic tree generation task. “Length” represents the length of the biological sequence (*e.g.*, the DNA sequence) of each species. See (Zhou et al., 2024) for details and references about these datasets. The number of species represents the number of nodes in the tree, and is a measure of complexity of the task.

Dataset	# Species (d)	Length
DS1	27	1949
DS2	29	2520
DS3	36	1812
DS4	41	1137
DS5	50	378
DS6	50	1133

C.2 Structure learning of Bayesian Networks

Given d continuous random variables (X_1, \dots, X_d) , a DAG G and parameters θ , a Bayesian Network represents the conditional independences in the joint distribution based on the structure of G

$$P(X_1, \dots, X_d; \theta) = \prod_{j=1}^d P(X_j | \text{Pa}_G(X_j); \theta_k), \quad (75)$$

where $\text{Pa}_G(X_j)$ represents the parent variables of X_j in G . We assume that all conditional distributions are linear-Gaussian. The objective of Bayesian structure learning is to approximate the posterior distribution over DAGs: $P(G | \mathcal{D}) \propto P(\mathcal{D} | G)P(G)$, where $P(\mathcal{D} | G)$ is the marginal likelihood and $P(G)$ is a prior over graph, assumed to be uniform here. Our experiments vary in the way the marginal likelihood is computed, either based on the BGe score (Geiger and Heckerman, 1994), or the linear Gaussian score (Nishikawa-Toomey et al., 2023). We followed the experimental setup of Deleu et al. (2022), where data is generated from a randomly generated ground truth Bayesian network G^* , sampled using an Erdős-Rényi scheme with on average 1 edge per node. We generated 100 observations from this Bayesian Network using ancestral sampling. We repeated this process for 20 different random seeds.

A state of the soft MDP corresponds to a DAG G over d nodes, and the initial state is the empty graph over d nodes. An action consists in adding a directed edge between two nodes, such that it is not already present in the graph, and it doesn’t introduce a cycle, guaranteeing that all the states of the MDP are valid acyclic graphs; there is a special action indicating whether we want to terminate and transition to s_f .

C.3 Phylogenetic tree generation

We consider the environment introduced by Zhou et al. (2024), where phylogenetic trees used for the analysis of the evolution of a group of d species are generated, according to a parsimonious criterion. Indeed, trees encoding few mutations are favored as they are more likely to represent realistic relationships. Given a tree T , whose nodes are the species of interest, the target distribution is given by

$$P(T) \propto \exp(-M(T | \mathbf{Y})/C), \quad (76)$$

where $C = 4$ is a fixed constant, and $M(T | \mathbf{Y})$ is the total number of mutations (also known as the *parsimony score*), based on the biological sequences \mathbf{Y} associated with each species; note that for convenience, we treat the energy function as being $\mathcal{E}(T) = M(T | \mathbf{Y})/C$ (with $\alpha = 1$). We used 6 out of the 8 datasets considered by Zhou et al. (2024); the statistics of the datasets are recalled in Table 2 for completeness.

A state of the soft MDP is a collection of trees over a partition of all the species (the leaves of the trees are species), where the initial state corresponds to d trees with a single node (leaf), one for each species in the group. An action consists in picking two trees, and merging them by adding a root. The process terminates when there is only one tree left in this collection, meaning that all complete trajectories have the same length $d - 1$. The size of the sample space is $(2d - 3)!!$ (for $d \geq 2$).

In addition to Figure 5, we also provide a complete view of the correlation between the terminating state log-probabilities and the returns for all algorithms and all datasets in Figures 7 & 8. Each point corresponds to a tree sampled using the terminating state distribution found by the corresponding algorithm.

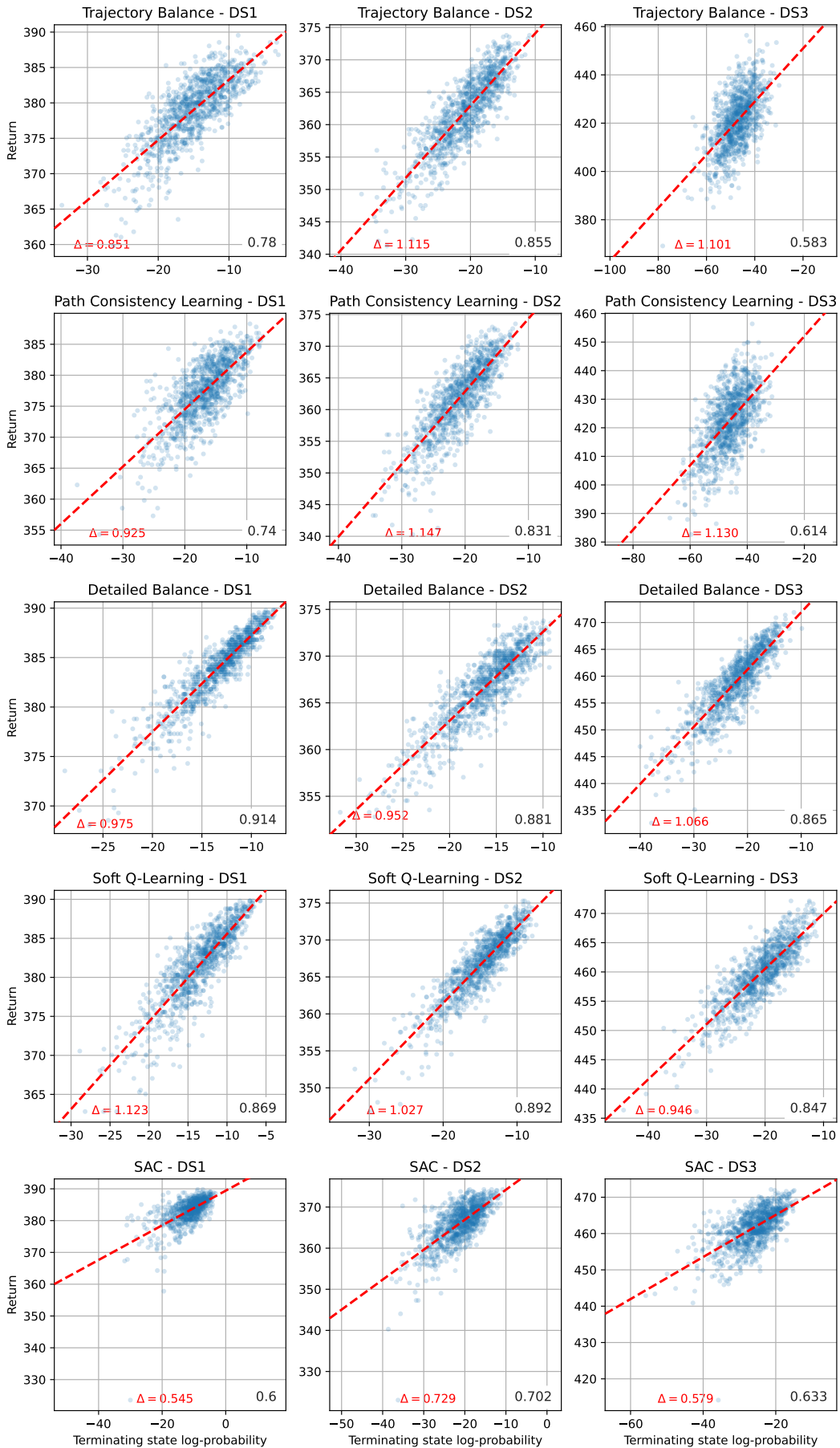


Figure 7: Correlation plots for all algorithms. Rows from top to bottom: Trajectory Balance (TB), Path Consistency Learning (PCL), Detailed Balance (DB), Soft Q-Learning (SQL) and SAC. Columns showing DS1 to DS3 from left to right.

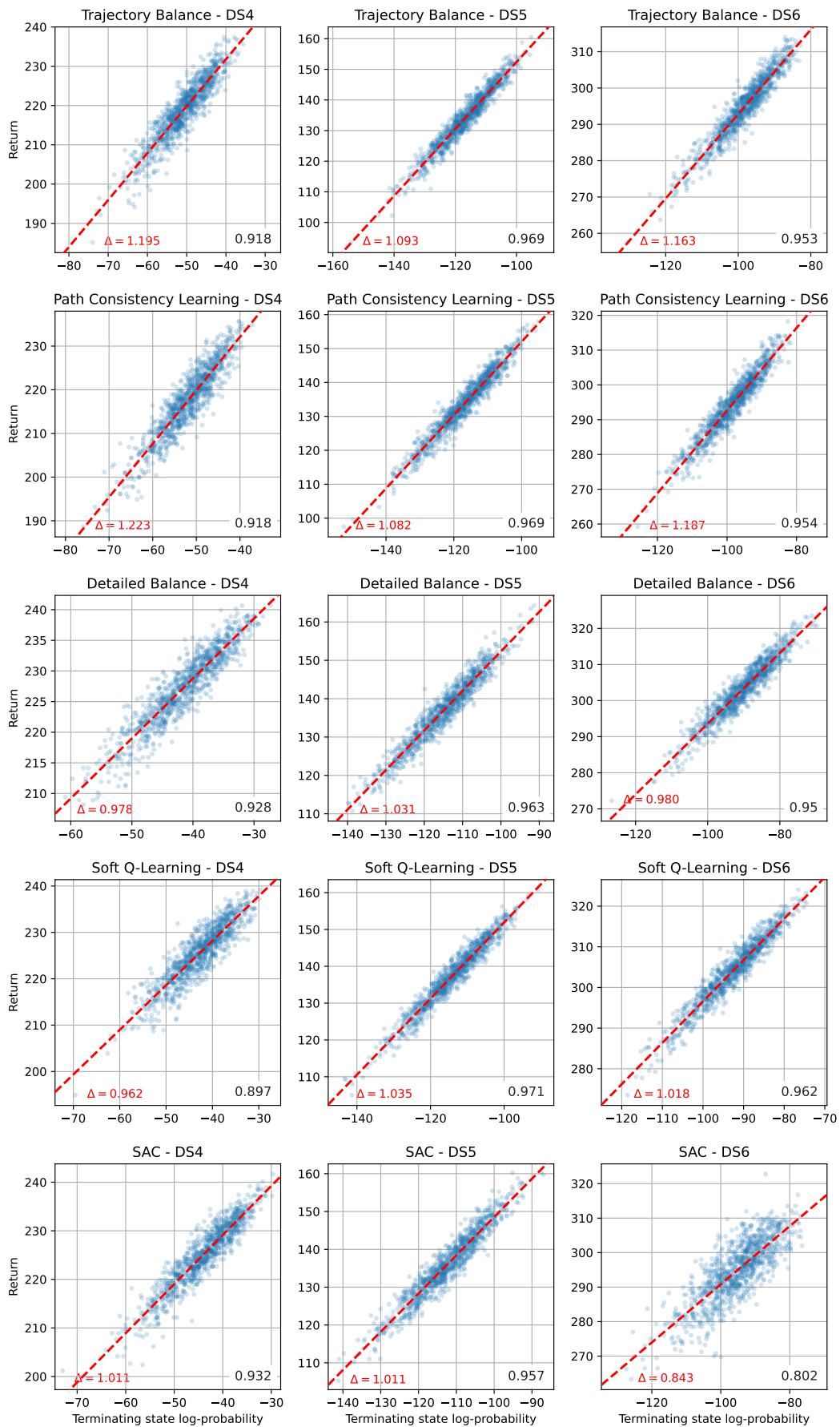


Figure 8: Similar plots as Figure 7 here columns presenting DS4, DS5 and DS6 from left to right.